

# **Analytical Solutions to Compartmental Indoor Air Quality Models with Application to Environmental Tobacco Smoke Concentrations Measured in a House\***

**Wayne R. Ott**

Departments of Statistics  
Stanford University  
Stanford, CA 94305

**Neil E. Klepeis**

Environmental Health Sciences  
School of Public Health  
University of California and  
Indoor Environment Department  
Lawrence Berkeley National Laboratory  
Berkeley, CA 94720

**Paul Switzer**

Departments of Statistics  
Stanford University  
Stanford, CA 94305

November 27, 2002

**Key Words:** Environmental Tobacco Smoke, Real-Time Measurements, Mass Balance Equation, Compartment Modeling, Laplace Transforms, Homes, Indoor Air Quality

---

\*This manuscript is a preprint for an article published in *Journal of the Air and Waste Management Association* 53(8) : 918-936, August 2003. It reflects changes made as of November 27, 2002, although there may have been other minor changes prior to final publication.

# Contents

<b>1</b>	<b>Introduction</b>	<b>3</b>
1.1	Single-Compartment Models . . . . .	4
1.2	Multi-Compartment Models . . . . .	6
<b>2</b>	<b>Two Compartment Model Derivation</b>	<b>8</b>
2.1	Laplace Transform for a Two Compartment Model . . . . .	11
2.2	Impulse Source Time Function and Natural Response . . . . .	11
2.3	Step, or Heaviside, Source Time Function . . . . .	13
2.4	Rectangular, or Double Heaviside, Source Time Function . . . . .	16
2.5	Single-Compartment Illustration . . . . .	17
<b>3</b>	<b>Model Evaluation: Experiments in a Home</b>	<b>20</b>
3.1	Spatial Variation Within a Bedroom . . . . .	22
3.2	Concentrations in Two Adjacent Rooms with Door Open . . . . .	26
3.3	Concentrations in Adjacent Rooms with Doors Almost Closed . . . . .	28
<b>4</b>	<b>Summary and Conclusions</b>	<b>32</b>
<b>A</b>	<b>Laplace Transforms of the Source Time Functions in this Paper</b>	<b>37</b>
<b>B</b>	<b>Laplace Approaches for Solving Differential Equations</b>	<b>38</b>

## Abstract

This paper derives solutions to multicompartment indoor air quality models for predicting indoor air pollutant concentrations in the home and evaluates the solutions using experimental measurements in the rooms of a single-story residence. The model uses Laplace transform methods to solve the mass balance equations for one compartment or two interconnected compartments, obtaining analytical expressions. Environmental tobacco smoke (ETS) sources such as the cigarette typically emit pollutants for relatively short times (7–11 min) and are represented mathematically by a "rectangular" source emission time function, a "step" function, or approximated by a short-duration source called an "impulse" time function. Other time-varying indoor sources also can be represented. The two-compartment models includes parameters for cigarette or combustion source emission rate as a function of time, room volumes, compartmental air change rates, and interzonal air flows. We evaluate the indoor model in an unoccupied two-bedroom home using cigars and cigarettes as sources with continuous measurements of carbon monoxide (CO), respirable suspended particles (RSP), and particulate polycyclic aromatic hydrocarbons (PPAH). In our experiments, simultaneous measurements of concentrations at three heights in a bedroom confirm an important assumption of the model, which is the spatial uniformity of mixing. The parameter values of the two-compartment model were obtained using a grid search optimization method, and the predicted solutions agreed well with the measured concentration time series in the rooms of the home. The door and window positions in each room had considerable effect on the pollutant concentrations observed in the home. Because of the small volumes and low air change rates of most homes, indoor pollutant concentrations from smoking activity in a home can be very high and can persist at measurable levels indoors for a number of hours.

## 1 Introduction

On average, Americans spend 69% of their time at home, 18% in other indoor locations (offices, stores, etc.), 5-6% in enclosed vehicles (buses, vans, automobiles, etc.), and 8% outdoors.<sup>1</sup> Many indoor sources of air pollution – smoking, cooking, consumer products, gas appliances, building materials – are found in homes. Despite the importance of the contribution of the home microenvironment to a person's total exposure to environmental pollutants, relatively few indoor air quality models have been applied to the home microenvironment or evaluated using experimental data from real homes.<sup>2</sup>

This paper applies a compartmental indoor air quality mass balance model to a detached, single-story house in Menlo Park, CA to predict the concentration time series from ETS in different rooms. The home was temporarily unoccupied, allowing a variety of experiments to be conducted with different combinations of source locations, monitoring locations, and door and window positions. We derive analytical solutions for the predicted concentration time series in different rooms, and evaluate the solutions using measurements of carbon monoxide (CO), respirable suspended particles (RSP), and polycyclic aromatic hydrocarbons (PAH).

Nearly all indoor air quality models<sup>2–17</sup> are based on the concept that mass released by an indoor source must be conserved, i.e., either the emitted mass remains in the air of the room, the mass leaves because it is carried through doors, windows, and cracks to other rooms or to the outdoors, or the mass is purged by indoor “sinks.” These models assume the air is sufficiently well-mixed due to indoor turbulence and other factors, so that the concentration is approximately the same everywhere in the room at any instant of time.<sup>15–17</sup> The mass balance assumptions of conservation of mass and uniform mixing permit a system of linear differential equations to be derived for indoor compartments. Miller and Nazaroff<sup>13</sup> have applied these approaches to cigarette smoking activity in the home, verifying model predictions with experimental data. This paper builds upon this prior research and extends the analytical solutions to cases not previously presented.

## 1.1 Single-Compartment Models

For sources lasting brief time periods, such as a single Marlboro cigarette smoked in the bedroom of a home in Redwood City, CA with the door closed (Figure 1), the interior pollutant concentrations rise rapidly, then show a gradual decay over several hours. The characteristic time series pattern of these plots follows closely the single-compartment solutions to the mass balance equation.<sup>3–17</sup> Solutions of the single-compartment mass balance are found in the literature.<sup>3,9,11,16</sup> In Figure 1, each curve after the cigarette has ended resembles an exponentially decaying function. An important parameter of this function is the “decay rate.” A related quantity is called the “residence time,” which is the reciprocal of the decay rate. Typical air change rates of homes range from 0.3 to 3 air changes per hour (ach).<sup>18,19</sup> If the time duration of the source is small compared with the “residence time,” then it may be possible to represent the source as a known mass of material emitted over a very short time interval, creating a high initial concentration in the room, or an “impulse” time function. A typical cigarette lasts 7–11 minutes, often much less than the residence time from residential air change rates and pollutant sinks, and thus Mage and Ott<sup>16</sup> suggest that the impulse’s conditions often are met for the cigarette in indoor settings. Some other indoor sources emit for longer durations, requiring other source time functions.

Few data are available on cigarette smoking time durations of people in real settings, but we observed the smoking activity of 33 persons in a Las Vegas casino a decade ago and found an average cigarette duration of 9.25 minutes (standard deviation of 2.25 minutes). Pandian *et al.*<sup>19</sup> report that the median air exchange rate for 1,482 homes in the Southwestern U.S. was 0.67 air changes per hour (ach), giving a home residence time of  $1/(0.67) = 1.5$  hours, or 90 minutes. Comparing these two studies, we discover that the ratio of the cigarette’s typical time duration to the median residence time was about 1:10, suggesting a representation of the cigarette as an impulse function, also called a Dirac delta function.<sup>20–28</sup>

In previous ETS research, Ott *et al.* applied the single-compartment mass balance model to cigarette smoking in a chamber and an automobile.<sup>9</sup> Klepeis *et al.* applied the model to public smoking lounges and found excellent agreement for CO and RSP be-

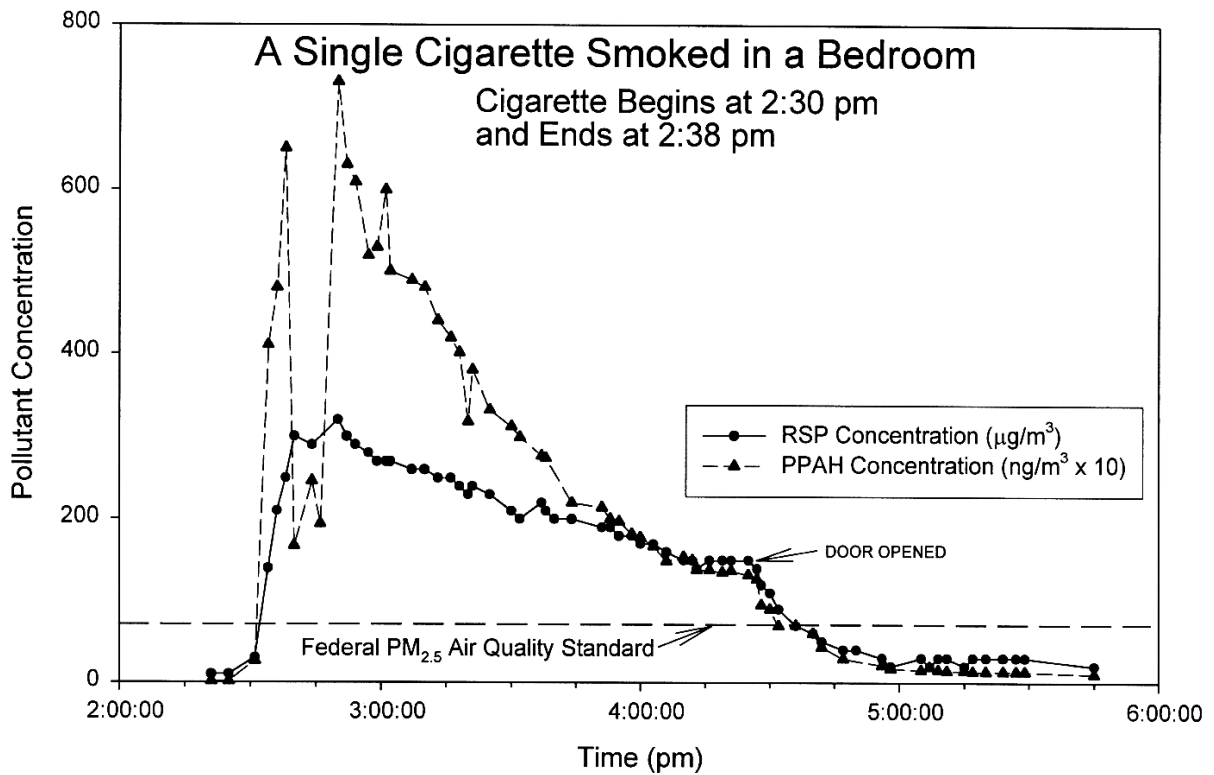


Figure 1: Measured respirable suspended particles (RSP or PM<sub>3.5</sub>) mass concentration and particulate polycyclic aromatic hydrocarbons (PPAH) in the bedroom of a home with the door closed after a single Marlboro regular filter cigarette was smoked. This home was located in Redwood City, CA and the models and experiments described in this paper were carried out in a another home in Menlo Park, CA. The federal air quality standard, which applies to a 24-hour averaging time period, could be exceeded indoors if multiple cigarettes are smoked each day in a home.

tween the predicted concentration time series and the observed concentrations measured with real-time monitors for two-minute averaging periods.<sup>10</sup> In another study, Ott et al. applied the same indoor model to a 521 m<sup>3</sup> sports bar in California<sup>11</sup> and found good agreement between the predicted average RSP concentrations on 76 visits lasting 0.3–2 hours each.

## 1.2 Multi-Compartment Models

Not all homes behave as a single compartment under all situations, and, therefore, more complicated indoor models must be considered. If a house contains many rooms, some with closed doors, it may be necessary to use a multi-compartment model rather than a single-compartment model. Although many indoor air quality models are discussed in the literature, few models have been applied to residences or tested with experimental data from real houses.

McKone<sup>4</sup> developed a three-compartment model to compute the 24-hour concentration history of Volatile Organic Compounds (VOCs) in the shower, bathroom, and remaining household volumes from tap water use. Wilkes *et al.*<sup>5</sup> used an indoor model implemented on a personal computer to show that daily inhalation exposure for a person with a contaminated water supply could exceed the person's daily ingestion exposure from the same tap water. Axley and Lorenzetti<sup>6</sup> used a multi-compartment indoor air quality modeling system based on commercially available software. Sparks *et al.*<sup>7</sup> developed a multi-compartment computer model for a home and verified the model for VOC sources such as wood stain, varnish, and floor wax. Indoor air quality models that can be used in homes are described in several books,<sup>2,8</sup> although few of these models have been applied using measurements of secondhand smoke as an indoor source.

The research papers by Miller, Leiserson, and Nazaroff<sup>12</sup> and by Miller and Nazaroff<sup>13</sup> are especially relevant, because they use a two compartment indoor model with measurements of tracer pollutants and ETS to evaluate the performance of this model. Our research extends their main findings by considering the step and rectangular source emission time functions. We use Laplace transform methods<sup>20–28</sup> to represent the source and to solve the mass balance equations. This approach gives analytical solutions that can be evaluated using a spreadsheet or hand calculator.

In this paper, we first derive the differential equations for two adjacent rooms by accounting for all the pollutant mass that either is emitted or contained in the interior air of the enclosed compartment of each well-mixed room. We omit deposition processes that apply to particles, although these sink processes can be easily added. Next we use Laplace methods to solve the two compartment model for impulse, step, and rectangular source functions of time, giving analytical solutions. Finally, we evaluate single and two compartment indoor air models using experimental data measured in a real home.

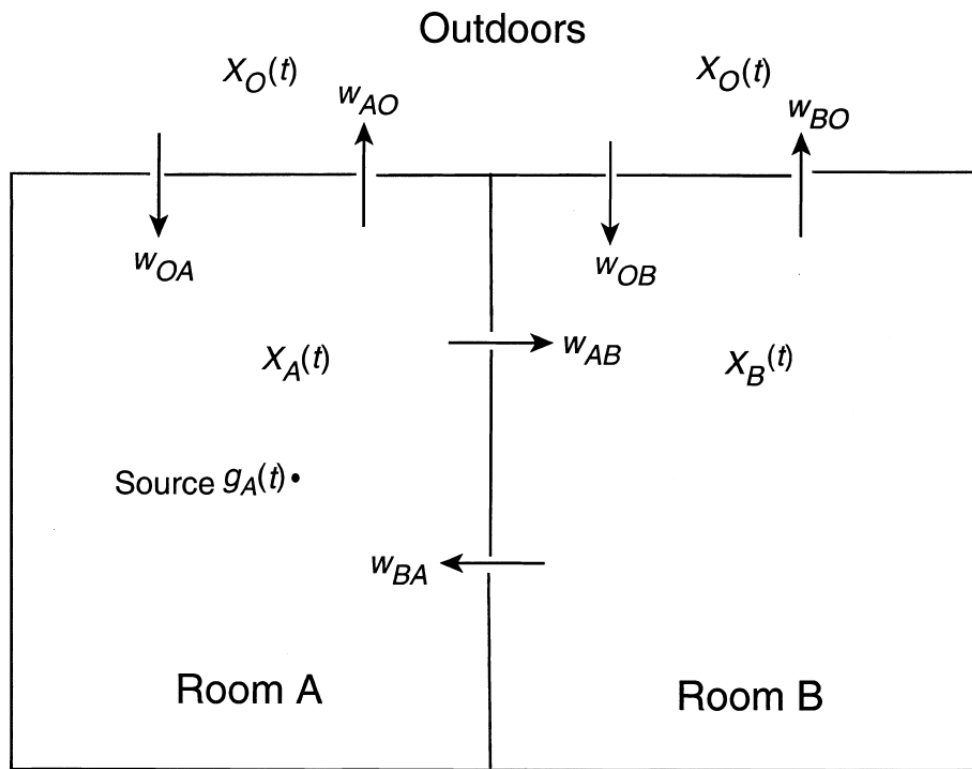


Figure 2: Simplified schematic of two adjacent rooms for a two-compartment indoor air quality model with a single source in Room A and arrows representing air flowing through a door or walls. The doors to the other rooms of the home are not shown and are assumed to be tightly sealed off, while the openings between the two adjacent rooms allow constant air flow rates  $w_{AB}$  and  $w_{BA}$  in either direction. There are also air flow rates  $w_{OA}$  and  $w_{AO}$  between Room A and the outdoors and air flow rates  $w_{OB}$  and  $w_{BO}$  between Room B and the outdoors. Each pair of flows are not necessarily equal, i.e., they may be unbalanced.

## 2 Two Compartment Model Derivation

Consider two adjacent rooms in a house in which “A” denotes a room containing a source and “B” denotes an adjacent room (Figure 2). Here, the subscript “AB” denotes the Room-A-to-Room-B air movement, “BA” denotes the reverse air movement. Thus,  $w_{AB}$  is the forward interzonal flow rate (volume of air per unit time, or units of  $L^3/T$ ), and  $w_{BA}$  is the reverse interzonal flow rate. The Outdoors-to-Room-A air flow rate is  $w_{OA}$ , which represents the air flowing into the windows from outdoors or seeping through cracks in the walls, and  $w_{AO}$  denotes the air flow rate from Room A to the outdoors. Similarly, the Outdoors-to-Room-B air flow rate is  $w_{OB}$  and the flow rate from Room B to outdoors is  $w_{BO}$ . By the principle of continuity of air flow in each room, the inflow and outflow rates must be the same:

$$w_{AO} + w_{AB} = w_{BA} + w_{OA} = w_A \quad (1)$$

$$w_{BO} + w_{BA} = w_{AB} + w_{OB} = w_B \quad (2)$$

In these analyses, we assume that the flow rates in Equations 1 and 2 remain constant over the full duration of the experimental time period under consideration. All flow rates in Figure 2 are positive quantities.

It is important to specify these flow rates in both directions, because air moving from indoors to outdoors from Room A at flow rate  $w_{AO}$  will carry the pollutant at concentration  $x_A(t)$  from the room itself to the outdoors, while air entering from outdoors into Room A at flow rate  $w_{OA}$  will carry the outdoor pollutant indoors at concentration  $x_O(t)$ . To consider the mass balance for Room A, we assume that the initial concentration for Room A is  $x_A(t) = 0$  at time  $t = 0$ . The positive terms for Room A on the left side of Equation 3 account for the total mass in Room A contributed by its interior source  $g_A(t)$  from  $t = 0$  to time  $t = T$ , the mass of pollutant entering into Room A from the adjacent Room B, and the mass of pollutant entering into Room A from outdoors. The negative terms on the left side of Equation 3 account for the total mass of pollutant lost from Room A to the adjacent room B and to the outdoors from time  $t = 0$  to time  $t = T$ . The sum of these quantities at time  $t = T$  equals the mass distributed within Room A’s air volume  $v_A$  at time  $t = T$ , or the total mass of  $v_A x_A(T)$  given on the right-hand side of Equation 3:

$$\begin{aligned} \text{Room A: } \int_0^T g_A(t)dt + \int_0^T w_{BA}x_B(t)dt - \int_0^T w_{AB}x_A(t) + \int_0^T w_{OA}x_O(t) - \int_0^T w_{AO}x_A(t) \\ = v_A x_A(T) \quad (3) \end{aligned}$$

$$\begin{aligned} \text{Room B: } \int_0^T w_{AB}x_A(t)dt - \int_0^T w_{BA}x_B(t) + \int_0^T w_{OB}x_O(t) - \int_0^T w_{BO}x_B(t) = v_B x_B(T) \quad (4) \end{aligned}$$

Equation 4 is similar to Equation 3, except that it applies to Room B, which does not contain a source, so the source term is absent. Determining the behavior of the concentration time series in each of the two rooms for a given source time series  $g_A(t)$  requires solving the pair of simultaneous differential equations given in Equations 3 and 4.

Differentiating Equations 3 and 4, and rearranging terms, we obtain:

$$v_A \frac{dx_A(t)}{dt} + (w_{AB} + w_{AO})x_A(t) = g_A(t) + w_{BA}x_B(t) + w_{OA}x_O(t) \quad (5)$$

$$v_B \frac{dx_B(t)}{dt} + (w_{BA} + w_{BO})x_B(t) = w_{AB}x_A(t) + w_{OB}x_O(t) \quad (6)$$

Overall, in addition to the source emission characteristics, the concentrations in Room A and Room B will be determined by two interzonal flow rate parameters, two external flow rate parameters, and the two room volumes. For the pair of attached rooms, therefore, there are four flow rate parameters and two physical mixing volumes, giving a total of six parameters, in addition to parameters describing the source. The form of the emission rate of the source with respect to time  $g_A(t)$  is important for determining the time series solutions in both rooms.

To facilitate the analysis, we introduce “normalized” parameter definitions. In the equations below, each room’s individual air change rate  $\phi_A$  and  $\phi_B$  is expressed as the number of air changes per unit time and the interzonal air flow factors  $\alpha_{AB}$ ,  $\alpha_{OB}$ ,  $\alpha_{BA}$ , and  $\alpha_{OA}$  are dimensionless ratios between 0 and 1 that describe the proportion of the air intake into the room that comes from the adjacent room or from outdoors:

$$\phi_A = \frac{w_{AB} + w_{AO}}{v_A} = \text{Air Exchange Rate in Room A [T}^{-1}\text{]} \quad (7)$$

$$\phi_B = \frac{w_{BA} + w_{BO}}{v_B} = \text{Air Exchange Rate in Room B [T}^{-1}\text{]} \quad (8)$$

$$\alpha_{AB} = \frac{w_{AB}}{w_{AB} + w_{OB}} = \text{Proportion of Room B's Intake Air Coming from Room A} \quad (9)$$

$$\alpha_{OB} = \frac{w_{OB}}{w_{AB} + w_{OB}} = \text{Proportion of Room B's Intake Air Coming from Outdoors} \quad (10)$$

$$\alpha_{BA} = \frac{w_{BA}}{w_{BA} + w_{OA}} = \text{Proportion of Room A's Intake Air Coming from Room B} \quad (11)$$

$$\alpha_{OA} = \frac{w_{OA}}{w_{BA} + w_{OA}} = \text{Proportion of Room A's Intake Air Coming from Outdoors} \quad (12)$$

From these definitions, it follows that  $\alpha_{BA} + \alpha_{OA} = 1$  and  $\alpha_{AB} + \alpha_{OB} = 1$ . From Equations 1 and 2, it follows that  $w_A = w_{BA} + w_{OA}$  is the total intake air flow entering Room A, and  $w_B = w_{AB} + w_{OB}$  is the total intake air flow entering Room B. The total intake air into both rooms is  $w = w_A + w_B - (w_{BA} + w_{AB}) = w_{OA} + w_{OB}$ . By conservation of mass flow, the total inflow  $w$  also equals the total outflow  $w = w_{OA} + w_{OB} = w_{AO} + w_{BO}$ . These equations allow expression of an overall air change rate for both rooms combined, or the global air change rate  $\phi = (w_{AO} + w_{BO}) / (v_A + v_B) = w / (v_A + v_B)$ .

Using the normalized parameters in Equations 7–12 and temporarily removing the ambient concentration  $x_O(t)$  to focus only on the indoor concentrations, Equations 5 and 6 can be simplified and rewritten as follows:

$$\frac{1}{\phi_A} \frac{dx_A(t)}{dt} + x_A(t) = \frac{1}{w_{BA} + w_{OA}} g_A(t) + \alpha_{BA} x_B(t) \quad (13)$$

$$\frac{1}{\phi_B} \frac{dx_B(t)}{dt} + x_B(t) = \alpha_{AB} x_A(t) \quad (14)$$

Note that it is possible to have values of our new normalized parameters that correspond to negative flow rates. Since we disallow negative flow rates in Equations 5 and 6, negative values should also be excluded in evaluated solutions of Equations 13 and 14. Negative flows can arise if, for example, the flow into Room B from Room A,  $\alpha_{AB}\phi_B v_B$ , exceeds the total flow out of Room A,  $\phi_A v_A$ .

A common way of approximating the solutions to these equations is by Runge-Kutta methods, in which a computer program calculates a sequence iterative steps at small time increments using the discrete versions of these equations,<sup>26</sup> and it is customary to represent these equations by matrix algebra (see, for example, Rogers<sup>14</sup>). As an alternative to the iterative Runge-Kutta computer approach, the Laplace transform approach<sup>26</sup> provides analytical solutions to the indoor compartmental differential equations (Appendix B), and more details are described in another report.<sup>30</sup>

Using Laplace transform methods, we can obtain analytical solutions for the concentration as a function of time in both rooms for a known time-varying source  $g_A(t)$  located in one room and for defined interzonal flow rates between the rooms. The Laplace transformation integral (see Appendix A) can be used to derive tables of ‘‘Laplace transforms’’ for a great variety of input time series  $x_A(t)$  that are useful for modeling indoor air quality and for other engineering problems. Two examples of Laplace transforms are used in this paper and given in the Appendix, with the methods described in greater detail elsewhere<sup>30</sup> and in reference textbooks such as Dorf and Bishop<sup>20</sup>, D’Azzo<sup>21</sup>, D’Azzo and Houpis<sup>22</sup>, Franklin *et al*<sup>23</sup>, Gujic’ and Lelic’<sup>24</sup>, and Nise<sup>25</sup>, Blanchard, Devaney, and Hall<sup>26</sup>, Bugl<sup>27</sup>, and Edwards and Penney.<sup>28</sup> The methodology is outlined briefly below, followed by the solutions for three common cases obtained using the Laplace transforms in the Appendix: the impulse, step, and rectangular source time functions.

## 2.1 Laplace Transform for a Two Compartment Model

The differential equations in Equations 13 and 14 can be solved simultaneously by the method of substitution. The first step is to solve Equation 14 for  $x_A(t)$  and take its derivative  $dx_A(t)/dt$ . Then both  $x_A(t)$  and  $dx_A(t)/dt$  are substituted into Equation 13, creating a second order differential equation containing only the variables  $d^2x_B(t)/dt^2$ ,  $dx_B(t)/dt$ , and  $x_B(t)$  for Room B and the source term  $g_A(t)$  for Room A. Using this approach, we derive the general two compartment Laplace transform for Room B's concentration time series as function of Room A's source input Laplace transform:

$$L\{x_B(t)\} = \frac{\alpha_{AB}\phi_A\phi_B}{w_{AB} + w_{AO}} \frac{1}{s^2 + s(\phi_A + \phi_B) + \phi_A\phi_B(1 - \alpha_{AB}\alpha_{BA})} L\{g_A(t)\} \quad (15)$$

This Laplace transform equation for the two compartment model is completely general for any time-varying source emission rate  $g_A(t)$  for which a source Laplace transform  $L\{g_A(t)\}$  is known<sup>30</sup>. To find the Laplace transform  $L\{x_B(t)\}$  of the solution for a particular source time function, we substitute the Laplace transform  $L\{x_A(t)\}$  for Room A's source function into Equation 15. Thus we obtain the Laplace transform  $L\{x_B(t)\}$  of the concentration in Room B directly from Equation 15, and taking its inverse Laplace transform  $L^{-1}\{x_B(t)\}$  gives the time series solution for the concentration in Room B. This approach recognizes that different concentration time series occur in the two rooms, all of which depend on the form of the source time function  $g_A(t)$  in Room A. The next three sections use this approach to obtain the two compartment solutions for three common indoor source time series: the impulse, step, and rectangular time functions.

## 2.2 Impulse Source Time Function and Natural Response

Some indoor sources are strong but emit pollutants for only a brief moment in time. For example, if a person cooks popcorn too long in a microwave oven, a rapid release of smoke particles and other pollutants occurs when the door of the microwave oven is opened. The emission time period may a few seconds or less. Under the idealized well-mixed assumption of the mass balance model, the pollutant must be treated as equally distributed throughout the room's mixing volume at the initial time  $t = 0$ . In practice, the well-mixed assumption often causes relatively small error, because an indoor pollutant "puff" spreads out quickly, filling a large mixing volume such as a kitchen or a home. Mathematical steps for treating this case are discussed below.

To model an indoor impulse source in Room A, consider initial conditions in which the total mass released  $m_{source}$  is distributed uniformly over the mixing volume  $v_A$  at time  $t = 0$ , giving an initial concentration in the room of  $x_A(0) = (m_{source})/v_A$ . Here,  $m_{source}$  is the "source strength," typically expressed in mass units of mg, because a source emission rate in mg/min is inappropriate for an instantaneous case. The natural solution [what is this?] of any differential equation<sup>20–28,30</sup> is obtained by setting its input Laplace transform to

$L\{g_A(t)\} = 1$ . The “natural solution” is defined as the basic response of the system instead of a specific response to a particular type of source input function.

Replacing the Laplace term  $L\{g_A(t)\}$  by unity in Equation 15, one obtains the Laplace transform of the time series solution of the concentration in Room B, or  $L\{g_A(t)\}$ . The denominator in Equation 15 contains a quadratic equation that is solved for the roots  $s_1$  and  $s_2$ , the eigenvalues of the system.<sup>30</sup> Next the method of partial fraction yields two separate Laplace transforms of the form of Equation 53 in the Appendix. Finally, writing the exponential solutions based on Equation 53 for each of the two Laplace transforms and forming their sum is equivalent to obtaining the inverse Laplace transform, giving the solution  $x_B(t) = L^{-1}\{x_A(t)\}$ . Once the solution  $x_B(t)$  for Room B is known, the solution for Room A is found directly by substituting  $x_B(t)$  and its derivative  $x_B'(t)$  into Equation 14 and solving for  $x_A(t)$ , yielding the following analytical solutions for Rooms A and B:

$$x_A(t) = \frac{m_{source}}{v_A(s_1 - s_2)} \{(s_1 + \phi_B)e^{s_1 t} - (s_2 + \phi_B)e^{s_2 t}\} \quad \text{for } t \geq 0 \quad (16)$$

$$x_B(t) = \frac{m_{source}\alpha_{AB}\phi_B}{v_A(s_1 - s_2)} (e^{s_1 t} - e^{s_2 t}) \quad \text{for } t \geq 0 \quad (17)$$

where

$$s_1 = -\frac{1}{2}(\phi_A + \phi_B) + \frac{1}{2}\sqrt{(\phi_A - \phi_B)^2 + 4\phi_A\phi_B\alpha_{AB}\alpha_{BA}} \quad (18)$$

$$s_2 = -\frac{1}{2}(\phi_A + \phi_B) - \frac{1}{2}\sqrt{(\phi_A - \phi_B)^2 + 4\phi_A\phi_B\alpha_{AB}\alpha_{BA}} \quad (19)$$

Equations 16 and 17, including the eigenvalues in Equations 18 and 19, are the same as those derived by Miller, Leiserson, and Nazaroff<sup>12</sup> and Rodgers<sup>14</sup> for an impulse source. The time series solution for Room A (Equation 16) is the difference between two exponential functions of time, with a initial condition of  $x_A(t) = (m_{source})/v_A$  at time  $t = 0$ . As  $t$  becomes increasingly large, Room A's concentration decays toward  $x_A(t) = 0$ . The time series solution in Room B (Equation 17) has an initial condition of  $x_B(t) = 0$  at time  $t = 0$  and a single maximum concentration at time  $t = t_{max}$ , after which it decays toward  $x_B(t) = 0$  as  $t$  becomes increasingly large:

$$t_{max} = \frac{1}{s_1 - s_2} \ln \left( \frac{s_2}{s_1} \right) \quad (20)$$

$$x_B(t_{max}) = \frac{m_{source}\alpha_{AB}\phi_B}{v_A(s_1 - s_2)} (e^{s_1 t_{max}} - e^{s_2 t_{max}}) \quad (21)$$

The exact time  $t_{max}$  and value of the maximum concentration  $x_B(t_{max})$  in Room B given by these equations can be used for interpreting time series graphs from indoor experiments.

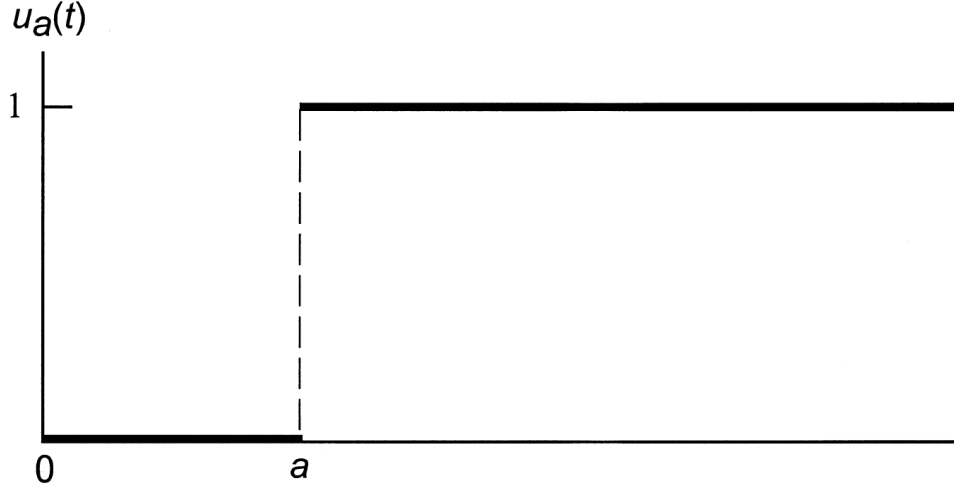


Figure 3: Heaviside or “step” function  $u_a(t)$  that is zero for time  $t < a$  and  $u_a(t)$  for  $t \geq a$ .

### 2.3 Step, or Heaviside, Source Time Function

Some indoor sources begin emitting at a particular time  $a$  and continue at a fixed emission rate for a long time period of many hours or even days. A burning incense stick has a reasonably constant emission rate over 3 hours or more. Prior to starting time  $t = a$ , the emission rate  $g(t)$  is zero for  $t < a$ . Thereafter, a constant emission rate of  $g_{source}$  occurs for time  $t \geq a$ . We represent this type of discontinuous “step” source function (Figure 3) using the Heaviside function  $u_a(t)$ , named after the engineer Oliver Heaviside<sup>26</sup> and defined as  $u_a(t) = 0$  for  $t < a$ , and  $u_a(t) = 1$  for  $t \geq a$ :

$$u_a(t) = \begin{cases} 0 & \text{for } t < a \\ 1 & \text{for } t \geq a \end{cases} \quad (22)$$

If the Heaviside function is multiplied by a source’s fixed emission rate  $g_{source}$ , giving  $g(t) = (g_{source})u_a(t)$ , this mathematical function will have zero emissions for  $t < a$  and will jump to a fixed value  $g(t) = g_{source}$  for  $t \geq a$ , remaining at the same emission rate  $g_{source}$  thereafter. As shown by Equation 52 in the Appendix, the Laplace transform for a step function source is  $L\{g_A(t)\} = 1/s$  if  $a = 0$ , which represents a source step function that begins emitting at  $t = 0$ , or  $g(t) = (g_{source})u_0(t)$ . Substituting this Laplace transform for the step time source function into Equation 15 for the two compartment model, solving the equations in the same manner as before, and taking the inverse Laplace transform of the result using the formulas in Appendix A gives the following solutions for the resulting time series in Rooms A and B for the step source function:

$$x_A(t) = \frac{g_{source}}{w_{AO} + w_{BO}\alpha_{AB}} \left( 1 + \frac{s_2(s_2 + \phi_A)e^{s_1 t} - s_1(s_1 + \phi_A)e^{s_2 t}}{(s_2 - s_1)\phi_B} \right) \quad \text{for } t \geq 0 \quad (23)$$

$$x_B(t) = g_{source} \frac{\alpha_{AB}}{w_{AO} + w_{BO}\alpha_{AB}} \left( 1 - \frac{s_2 e^{s_1 t} - s_1 e^{s_2 t}}{s_2 - s_1} \right) \quad \text{for } t \geq 0 \quad (24)$$

The first derivatives of the concentrations in Rooms A and B for the step source, also needed in the next section, are readily derived from these analytical solutions:

$$x'_A(t) = \frac{dx_A(t)}{dt} = g_{source} \frac{1}{w_{AO} + w_{BO}\alpha_{AB}} \frac{s_1 s_2}{s_2 - s_1} \left\{ \left( \frac{s_2}{\phi_B} + 1 \right) e^{s_2 t} - \left( \frac{s_1}{\phi_B} + 1 \right) e^{s_1 t} \right\} \quad \text{for } t \geq 0 \quad (25)$$

$$x'_B(t) = \frac{dx_B(t)}{dt} = g_{source} \frac{\alpha_{AB}}{w_{AO} + w_{BO}\alpha_{AB}} \left( \frac{s_1 s_2}{s_2 - s_1} [e^{s_2 t} - e^{s_1 t}] \right) \quad \text{for } t \geq 0 \quad (26)$$

Several analytical expressions derived from these equations are useful for interpreting measurement data from indoor experiments. For example, if a step source function begins in Room A at time  $t = 0$ , for example, then Room A's concentration has an initial slope at time  $t = 0$  given by:

$$x'_A(0) = \frac{g_{source}}{w_{AO} + w_{BO}\alpha_{AB}} \phi_A (1 - \alpha_{AB}\alpha_{BA}) \quad (27)$$

After this initial slope at  $t = 0$ , the slope  $x'_A(t)$  monotonically decreases with time. As  $t$  increases without limit, Room A's concentration has an asymptote given by:

$$\lim_{t \rightarrow \infty} \{x_A(t)\} = g_{source} \frac{1}{w_{AO} + w_{BO}\alpha_{AB}} \quad (28)$$

Room B's concentration  $x_B(t)$  begins with a slope of zero at  $t = 0$  (see  $x'_B(t)$  in Equation 26), and  $x_B(t)$  has a point of inflection  $t_f$  that depends on the system's eigenvalues  $s_1$  and  $s_2$ :

$$t_f = \frac{1}{s_1 - s_2} \ln \left( \frac{s_2}{s_1} \right) \quad (29)$$

The eigenvalues determine the exact time of the point of inflection for the concentration in Room B caused by the source function in Room A. As we see in the following section, the eigenvalues also are important for determining the time that a maximum concentration occurs in Room B when a rectangular source function occurs in Room A.

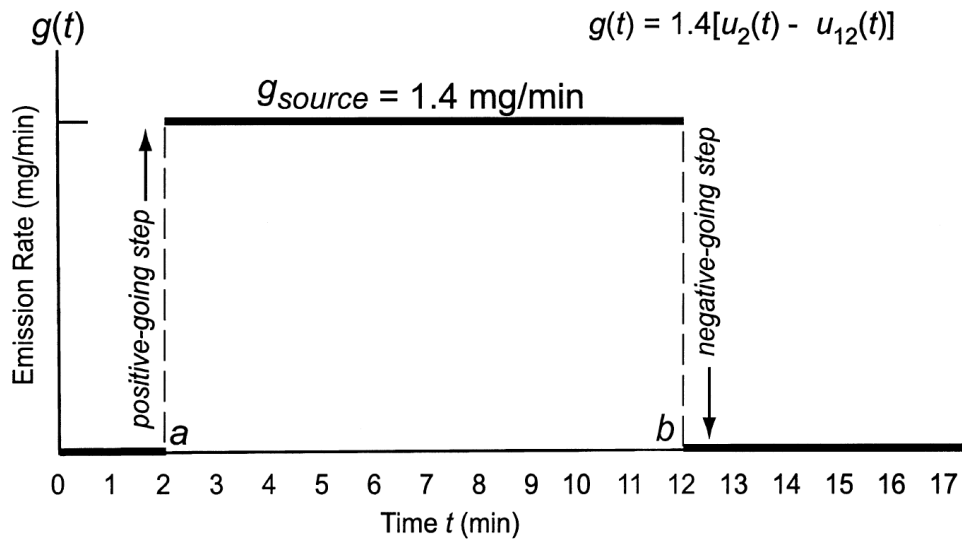


Figure 4: Rectangular source function for representing an indoor source that has zero emissions of RSP for time  $t < 2$  min and constant emission rate  $g(t) = g_{source} = 1.4$  mg/min for time  $2 \leq t < 12$  min, followed by a zero emission rate for time  $t \geq 12$ . This example might represent the fine particle source emission rate for a filter cigarette smoked for 10 min, showing the positive-going and negative-going Heaviside functions used to create a rectangular source function

## 2.4 Rectangular, or Double Heaviside, Source Time Function

Most indoor sources, such as a cigarette, continue emitting for a finite time period and then stop. Suppose a cigarette begins emitting at time  $t = 2$  and ends at  $t = 12$  min. This source time function consists of the sum of two Heaviside functions,  $u_2(t)$  and  $-u_{12}(t)$ , and the product of the cigarette's source emission rate  $g_{source} = g_{cig}$  (Figure 4). The first "positive-going" function  $(g_{cig})u_2(t)$  is the beginning emission of the cigarette and the second "negative-going" Heaviside function  $(g_{cig})u_{12}(t)$  is the end of the cigarette emission period, with an assumed RSP emission rate of 1.4 mg/min:

$$g(t) = (g_{cig})[u_a(t) - u_b(t)] = 1.4[u_2(t) - u_{12}(t)] \quad (30)$$

This double Heaviside function also is called a "rectangular" source function.

Although a cigarette may last 10 minutes until it burns out, a cigar may last 50 minutes or more<sup>29</sup>. Cigarette and cigar emission rates may vary as the smoker puffs, causing pollutant emissions to vary slightly with time, but approximating the emission as a rectangular sources often works well in practice. For a rectangular source beginning at  $t = 0$  and ending at  $t = b$ , the solutions in Rooms A and B over the time  $0 \leq t < b$  are the same as for the step function (Equations 23 and 24). At the emission stopping time  $t = b$ , the following equations give concentration time series in Rooms A and B for  $t \geq b$ :

$$x_A(t) = \frac{x_B(b)}{\alpha_{AB}\phi_B(s_1 - s_2)} \left\{ (s_2 + \phi_A)s_2 e^{s_1[t-b]} - (s_1 + \phi_A)s_1 e^{s_2[t-b]} \right\} \\ + \frac{x'_B(b)}{\alpha_{AB}\phi_B(s_1 - s_2)} \left\{ (s_1 + \phi_A)e^{s_2[t-b]} - (s_2 + \phi_A)e^{s_1[t-b]} \right\} \quad \text{for } t \geq b \quad (31)$$

$$x_B(t) = \frac{1}{s_1 - s_2} \left( e^{s_1[t-b]} - e^{s_2[t-b]} \right) [(\phi_A + \phi_B)x_B(b) + x'_B(b)] \\ + \frac{1}{s_1 - s_2} \left( s_1 e^{s_1[t-b]} - s_2 e^{s_2[t-b]} \right) x_B(b) \quad \text{for } t \geq b \quad (32)$$

In summary, Equations 23 and 24 describe the concentration solutions in Rooms A and B for the first part of a rectangular source beginning at  $t = 0$ , and Equations 31 and 32 describe the concentrations after the source stops emitting at time  $t \geq b$ . At  $t = b$ , the concentration  $x_A(b)$  and the slope  $x'_A(b)$  from Equation 23 and 25 are used in Equation 31 for Room A, and the concentration  $x_B(b)$  and the slope  $x'_B(b)$  from Equations 24 and 26 are used in Equation 32 for Room B. Because each room has two continuous concentration time functions joined at the point  $t = b$ , we call each room's equations "piecewise continuous" concentration time functions.

For the rectangular source function in Room A, Room A's maximum concentration occurs at time  $t = b$ . Room B's maximum concentration occurs after Room A's maximum concentration, causing a "time delay" in the maxima. By differentiating Equation 32 and

setting the derivative to zero, we obtain a useful expression for the time of the maximum concentration  $t_{max}$  in Room B:

$$t_{max} = \frac{1}{s_1 - s_2} \ln \left( \frac{F_1 s_2 + F_2 s_2^2}{F_1 s_1 + F_2 s_1^2} \right) + b \quad (33)$$

where  $F_1 = (\phi_A + \phi_B)x_B(b) + x'_B(b)$  and  $F_2 = x_B(b)$ . Substituting Room B's maximum concentration time  $t_{max}$  from Equation 33 into Equation 32 gives the predicted value of the maximum concentration in Room B.

We illustrate the characteristic shapes of these two compartment solutions for a rectangular source by an example in which a cigar emits carbon monoxide (CO) in the kitchen of a home (Room A), and the concentration is predicted for the adjacent living room (Room B) using Equations 23, 24, 31, and 32 (Figure 5). In this example, we assume a cigar Room A and emits CO at a rate of 70.6 mg/min (70,600  $\mu$ g/min) and burns uniformly for 15 min. The door between Room A and Room B is open only a few inches, restricting the air flow between the kitchen and living room, thus causing the rooms to behave as two compartments. This example of a cigar as a rectangular source time function uses the following values for the 6 physical parameters: kitchen and living room volumes  $v_A = 34$  m<sup>3</sup> and  $v_B = 36$  m<sup>3</sup>; air change rates  $\phi_A = 4.65$  air changes per hour (ach) and  $\phi_B = 4.17$  ach; and interzonal flow factors  $\alpha_{AB} = 0.614$  and  $\alpha_{BA} = 0.976$ . These parameter values are similar to those obtained using experiments in a house as described later in this paper.

At time  $t = 0$ , Figure 5 shows the concentration in Room A in this example rising sharply, with a much more gradual concentration increase in Room B. In Room A, the predicted maximum concentration occurs at time  $t = 15$  min, the ending time of the cigar emissions. In Room B, the predicted maximum concentration occurs at time  $t = 26.96$  min using Equation 33, or 11.96 min after the maximum concentration in Room A, illustrating the time delay of the maximum in the second room. Later in this paper, we compare the predicted two compartment solutions for a rectangular source with the experimental measurement results for a cigar smoked in the kitchen, living room, and bedroom of a real home.

## 2.5 Single-Compartment Illustration

The familiar solutions for step and rectangular sources in a single compartment also can be obtained by Laplace transforms, and the approach is illustrated here briefly. Equation 13 for the two compartment model can be converted into a single-compartment model for Room A by eliminating the interzonal flow between Room A and Room B by setting  $w_{BA} = 0$  and  $\alpha_{BA} = 0$ :

$$\frac{1}{\phi_A} \frac{dx_A(t)}{dt} + x_A(t) = \frac{1}{w_{OA}} g_A(t) \quad (34)$$

Following the rules for solving differential equations by Laplace transforms (Appendix B) and solving for the Laplace transform  $X_A(s)$  of Room A's concentration, where  $G_A(s)$

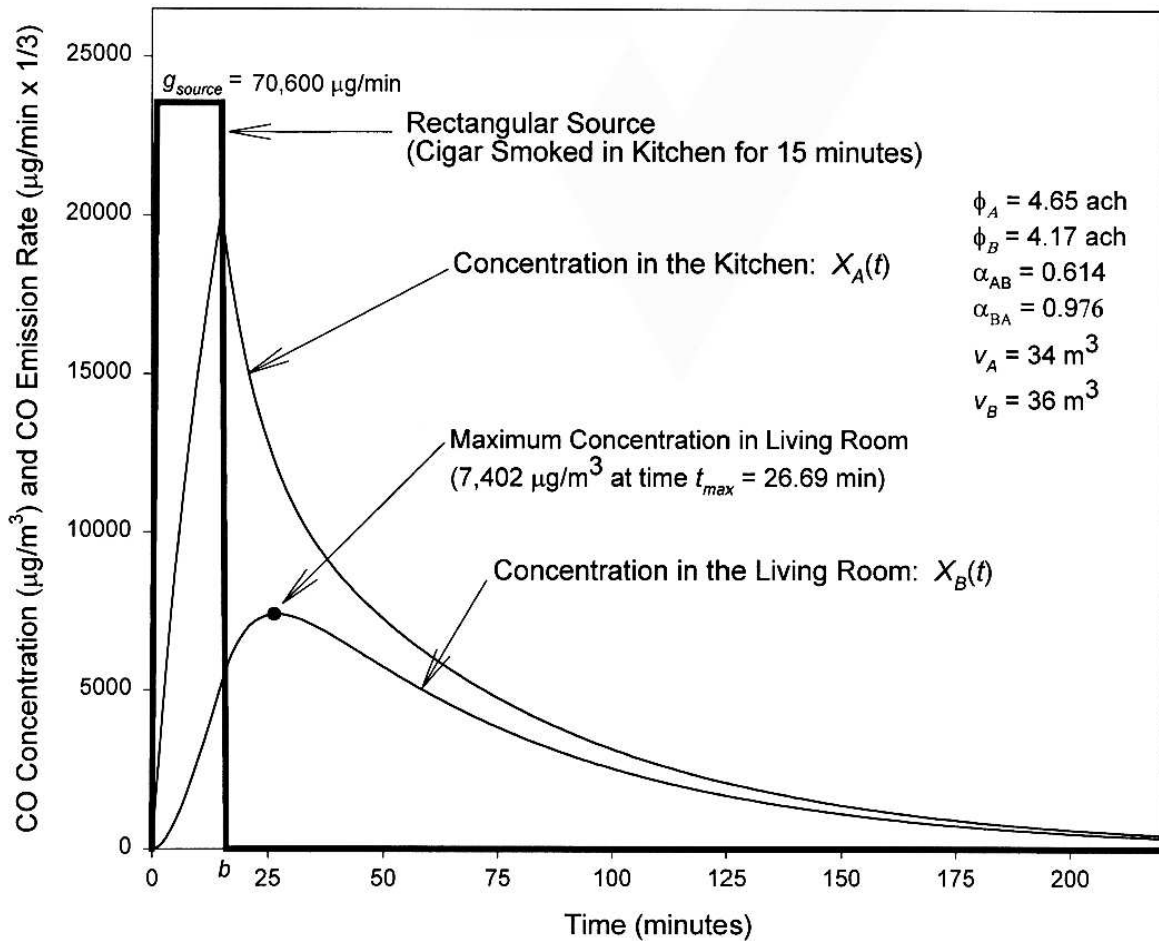


Figure 5: Example showing theoretical solutions to the two-compartment indoor model for a rectangular time series source in Room A, the kitchen. The source ends at time  $b = 15 \text{ min}$ , and the analytical solution in each room consists of the difference between two piecewise-exponential functions. The eigenvalues for the solutions in this example are  $s_1 = 0.9924 \text{ h}^{-1}$  and  $s_2 = -7.827 \text{ h}^{-1}$ .

represents the Laplace transform of the emission rate  $g_A(t)$  as a function of time gives the following general Laplace transform solution for the single-compartment model with initial conditions  $x_A(0)$ :

$$L\{x_A(t)\} = X_A(s) = \frac{\phi_A}{w_A} \frac{G_A(s)}{s + \phi_A} + \frac{x_A(0)}{s + \phi_A} \quad (35)$$

For a step source function with a constant emission rate  $g_{source}$  beginning at  $t = 0$ , we substitute  $G_A(s) = 1/s$  as before:

$$X_A(s) = \frac{\phi_A}{(s + \phi_A)w_{OA}} G(s) + \frac{x_A(0)}{s + \phi_A} = \frac{\phi_A}{w_A} \frac{g_{source}}{s(s + \phi_{OA})} + \frac{x_A(0)}{s + \phi_A} \quad (36)$$

Because no prior indoor sources are present, the initial condition is  $x_A(0) = 0$  and the far right-hand term in Equation 36 disappears. The remaining terms in Equation 36 are expanded by partial fractions:

$$X_A(s) = \frac{g_{source}\phi_A}{s(s + \phi_A)w_{OA}} = \frac{g_{source}}{s w_{OA}} - \frac{g_{source}}{(s + \phi_A)w_{OA}} \quad (37)$$

The right-hand side of Equation 37 contains the same two Laplace transforms derived in Appendix A with scaling factor  $g_{source}/w_{OA}$ . The term containing  $1/s$  is the Laplace transform of the Heaviside function and the term containing  $1/(s + \phi_A)$  is the Laplace transform of an exponential function with decay parameter  $\alpha = \phi_A$ . Using the relationships in Appendix A is equivalent to taking the “inverse Laplace transform” of Equation 37 by inspection:

$$L^{-1}\{X_A(s)\} = x_A(t) = \frac{g_{source}}{w_{OA}} u_0(t) - \frac{g_{source}}{w_{OA}} e^{-\phi_A t} u_0(t) = \frac{g_{source}}{w_{OA}} (1 - e^{-\phi_A t}) u_0(t) \quad (38)$$

This familiar indoor solution usually is written without its Heaviside notation:

$$g(t) = \frac{g_{source}}{w_{OA}} (1 - e^{-\phi_A t}) \quad \text{for } t \geq 0 \quad (39)$$

Equation 39 has been used in research on ETS sources to characterize the indoor concentrations of CO and particulate matter measured for a cigar in a tavern<sup>16</sup> and a home.<sup>29</sup> This model agreed well with measurements of CO and particles from cigarettes in a chamber and an automobile during the period in which the cigarette was burning.<sup>9</sup>

For a rectangular source of a nonreactive pollutant without major sinks that starts emitting at  $t = 0$  and ends at time  $t = b$ , the parameter  $\phi_A$  is the air exchange rate, often denoted in the literature as “ $a$ ” and expressed in air changes per hour (ach or hours<sup>-1</sup>). Equation 39 can be written using another useful parameter, the residence time  $\tau = 1/\phi_A$ , or the amount of time required for one full room volume  $v_A$  of air to be replaced:

$$x_A(t) = \frac{g_{source}}{w_{OA}} (1 - e^{-t/\tau}) \quad \text{for } 0 \leq t < b \quad (40)$$

For  $b \leq t$ , the concentration decays exponentially with time:

$$x_A(t) = \frac{g_{source}}{w_{OA}}(1 - e^{-b/\tau})e^{(t-b)/\tau} = x_A(b)e^{(t-b)/\tau} \quad \text{for } b \leq t \quad (41)$$

The maximum concentration  $x_A(\max)$  occurs at the exact time  $t = b$  when the emission source ends:

$$x_A(\max) = x_A(b) = \frac{g_{source}}{w_{OA}}(1 - e^{-b/\tau}) \quad (42)$$

Representing  $e^{-b/\tau}$  in Equation 42 as a Taylor expansion, and omitting terms raised to a power of 2 and higher gives a useful approximation for the case when the source duration  $b$  that is small compared with the residence time  $\tau$ :

$$x_A(\max) = \frac{g_{source}}{w_{AO}} \left\{ 1 - 1 + \frac{b}{\tau} - \frac{1}{2!} \left(\frac{b}{\tau}\right)^2 + \frac{1}{3!} \left(\frac{b}{\tau}\right)^3 - \dots \right\} \cong \frac{(g_{source})b}{w_{OA}\tau} \quad (43)$$

For any source emitting at a constant rate  $g_{source}$  over a time duration  $b$ , the total mass emissions generated will be  $m_{source} = (g_{source})b$ , and we can therefore substitute the source strength  $m_{source}$  for the product shown in the numerator in Equation 43. Substituting  $w_{AO} = w_{OA} = \phi_A v_A = v_A/\tau$  from Equation 7 for a single compartment (where  $w_{AB} = w_{BA} = 0$ ) into the denominator in Equation 43 yields a useful practical result:

$$x_A(\max) \cong \frac{m_{source}}{(v_A/\tau)\tau} = \frac{m_{source}}{v_A} \quad (44)$$

Thus, if  $b \ll \tau$  for the single-compartment case, then the maximum concentration in the room is approximately equal to the mass emitted  $m_{source}$  divided by the volume of the room  $v_A$ . This result is like imagining the mass emitted by the source to be uniformly distributed in the air volume  $v_A$  at or near the initial time  $t = 0$ , giving a predicted maximum concentration  $(m_{source})/v_A$  for a single compartment that decays exponentially for  $t > 0$  at decay rate  $\phi_A$ . Interestingly, the two compartment model in Equation 16 with an impulse source also yields the same initial concentration  $x_A(\max) = (m_{source})/v_A$  at  $t = 0$  in Room A as in Equation 44.

This approximation has a practical application in both one- and two compartment indoor air quality experiments. If the source emits for a short time period relative to the air residence time of the room, and if its maximum concentration  $x_A(\max)$  can be determined by experiment, then the source strength can be calculated approximately as the product of the room's volume  $v_A$  and the observed maximum concentration  $x_A(\max)$ :

$$m_{source} \cong v_A \cdot x_A(\max) \quad (45)$$

### 3 Model Evaluation: Experiments in a Home

To evaluate how well compartmental indoor air models predict the time series of concentrations for a cigarette smoked in a real home, we conducted more than 40 experiments

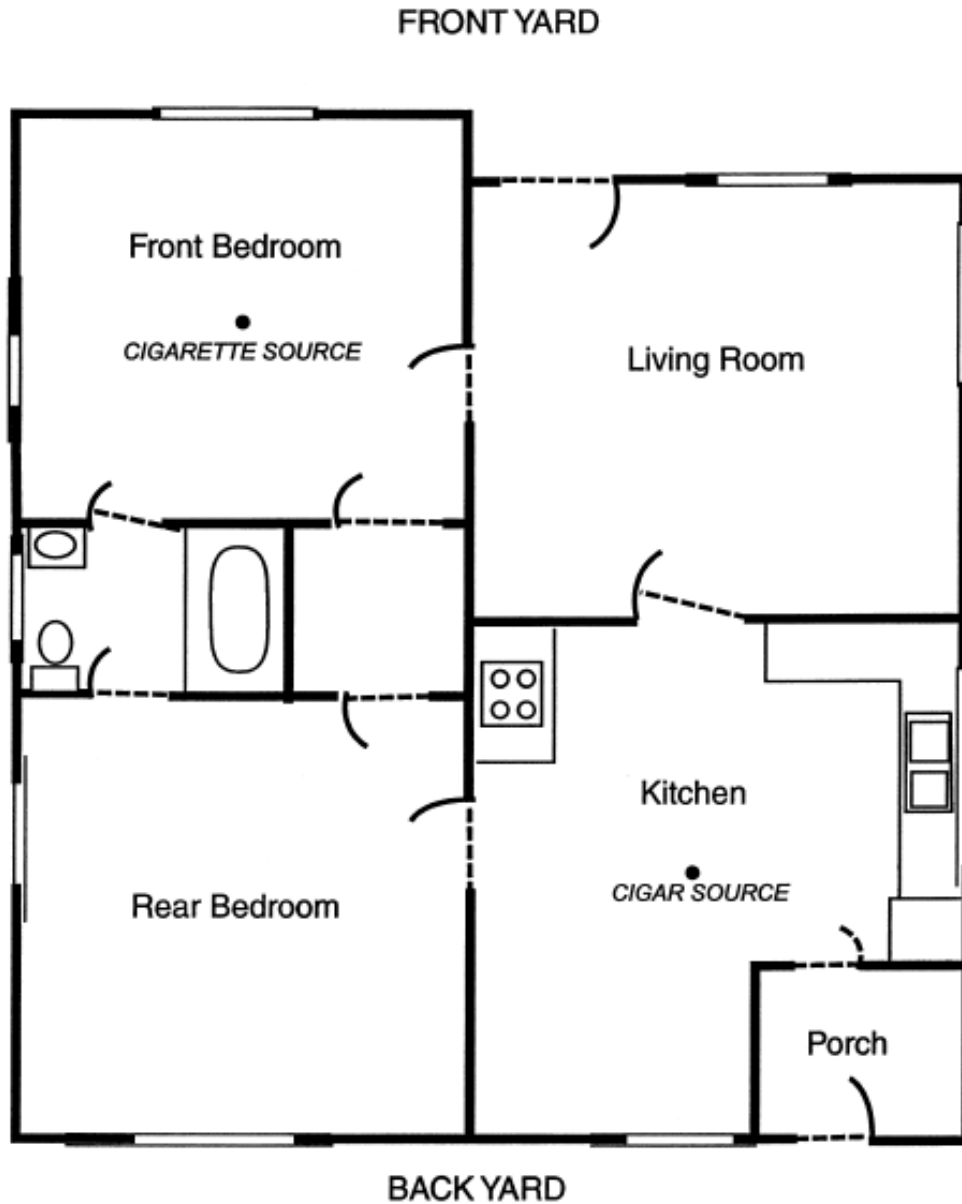


Figure 6: Floor plan of a two bedroom house in Menlo Park, CA used for indoor air quality experiments. There was no heating or ventilation system operating during the experiments.

in a detached single-story, two-bedroom house with outside dimensions of 28 ft by 24 ft, or 672 ft<sup>2</sup> (62.5 m<sup>2</sup>) on Partridge Ave. in Menlo Park, CA (Figure 6). The house was awaiting a new tenant and was not occupied, and we varied the locations of the monitors and the door and window positions in a variety of configurations. The sources tested included Marlboro regular filter cigarettes, University of Kentucky 2R1 research cigarettes, and cigars. The Kentucky 2R1 cigarettes are standardized for research and are stronger than commercially available cigarettes.

Selected results from these experiments were used to: (1) study the spatial variation of CO concentrations inside a single room of the residence (the bedroom), verifying the well-mixed assumption, and calculate a cigarette mass emission rate; (2) observe how pollutant concentrations (RSP, PAH, CO) vary in two connected rooms of the residence (bedroom and living room); and (3) evaluate the equations developed in the previous section for predicting CO concentrations observed in a pair of rooms – the kitchen and living room.

### 3.1 Spatial Variation Within a Bedroom

An important assumption of the mass balance model (Equations 3 and 4) is that, for any time  $t$ , the room is sufficiently well-mixed to give nearly the same concentration at all locations. To evaluate this assumption, we made measurements at three widely spaced locations in the 907.5 ft<sup>3</sup> (25.7 m<sup>3</sup>) bedroom of this house<sup>1</sup>: (1) near the floor in the corner of the room; (2) on a short step ladder 36" high in the center of the room; and (3) on a tall ladder 8.5" from the ceiling (Figure 7). CO concentrations were measured using a Langan L15 CO Personal Exposure Measurer<sup>31</sup> (Langan Products, San Francisco, CA). Each CO sensor was connected by a wire to a DataBear<sup>TM</sup> data logger which logged the data at 30-second intervals. For each CO sensor, a precision electronic operational amplifier multiplied the signal by 10.0 to increase the numerical resolution, and concentrations were measured at high sensitivity<sup>31</sup> and reported in parts-per-ten-million (pptm). Note that 10 pptm is 1 ppm CO.

Over a period of 16 hours, three Marlboro regular filter cigarettes were smoked in the center of the bedroom at a 36" height with the doors closed and with one window partly open but covered with a shade. The first cigarette was smoked just after noon (12:46:30 pm) and lasted for 6 minutes and 30 seconds; the exponential decay of the CO concentrations from this cigarette was quite similar for all three locations and lasted approximately 4.25 hours until just before 5:00 pm (Figure 8). The second cigarette began approximately at 5:00 pm and lasted for 7 minutes and 16 seconds; it generated an exponential decay curve at each of the three locations, although the concentration at the corner floor was lower than the concentration time series at the center of the room or at the ceiling. Finally, a third Marlboro cigarette was smoked at 9:56 pm for 9-1/2 minutes, and its exponential decay was observed until 3:49 am.. The air exchange rate was determined by subtracting the background concentration and taking the logarithms; the slope of the resulting

---

<sup>1</sup>These data have been previously analyzed by Klepeis (1999).<sup>17</sup>

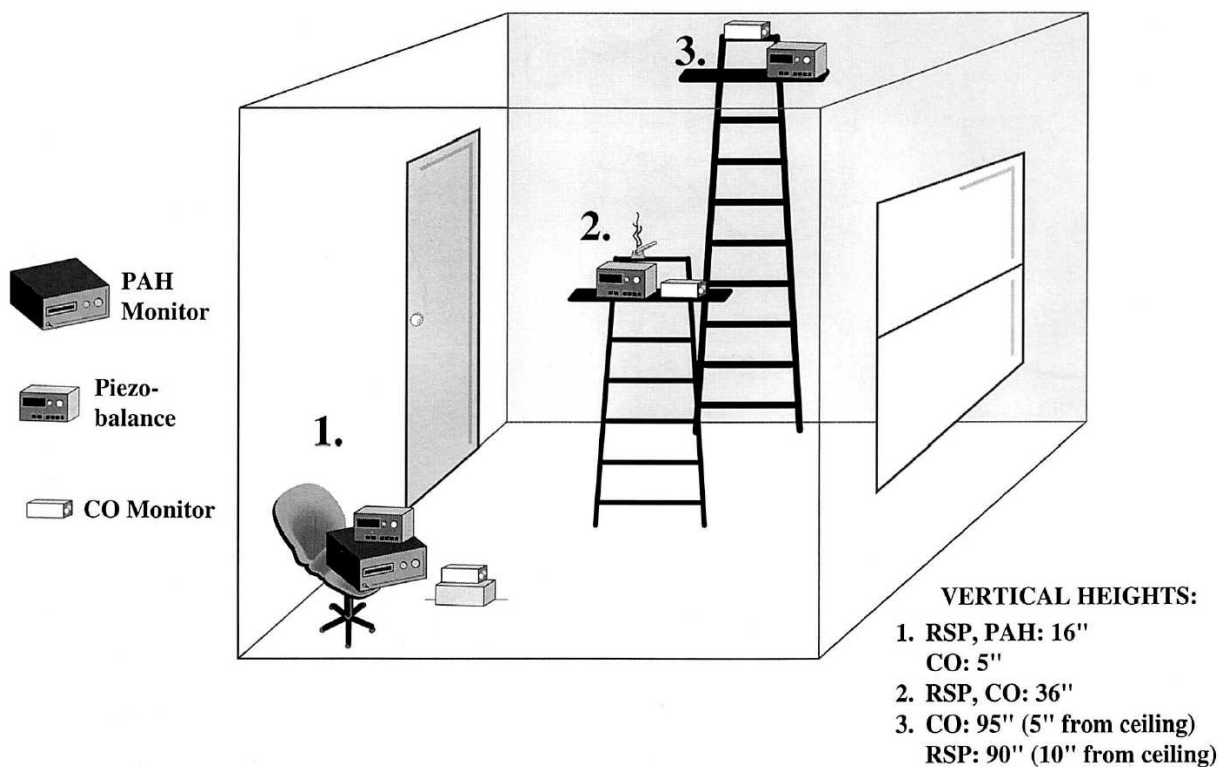


Figure 7: Location of monitor positions in the bedroom ( $v = 25.7 \text{ m}^3$ ) of the four-room house in Menlo Park, CA in which experiments were conducted to determine the spatial variation of indoor concentrations caused by smoking a cigarette.

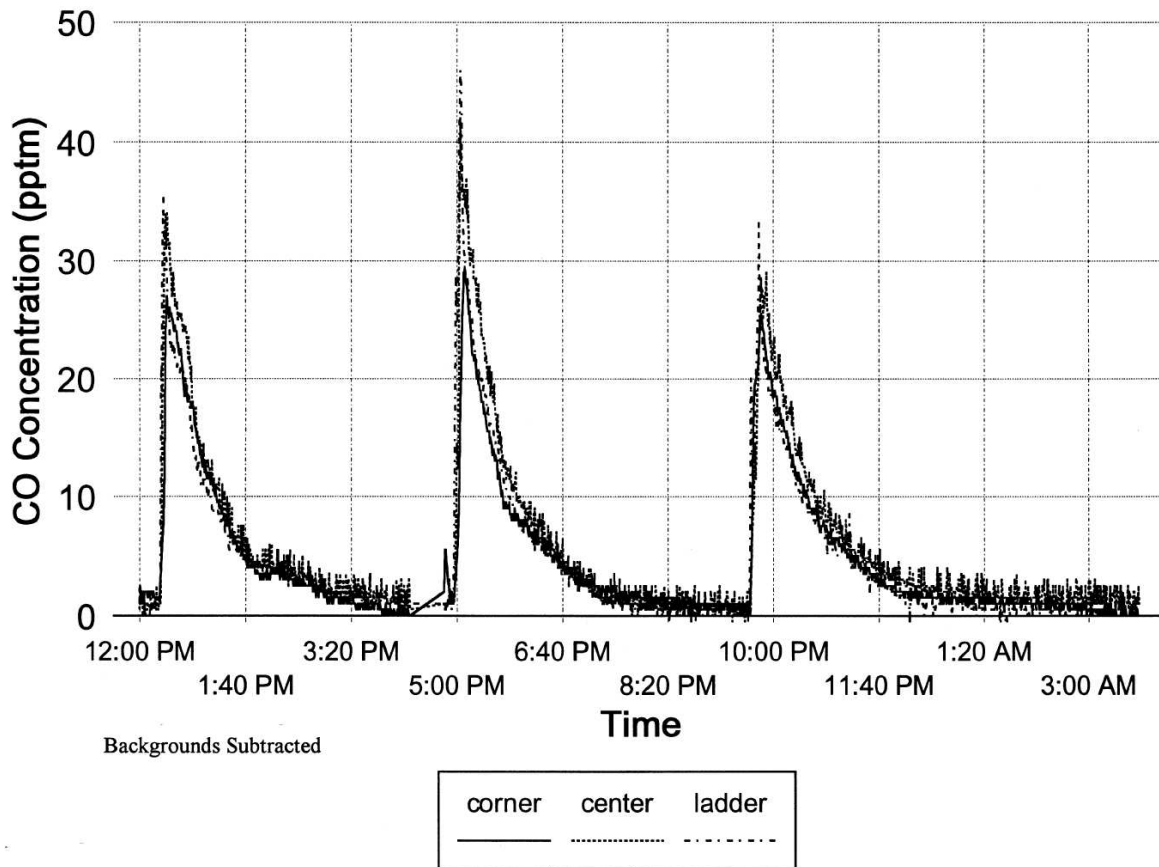


Figure 8: Carbon monoxide (CO) concentrations measured at three locations in a 25.7 m<sup>3</sup> bedroom over a 16-hour period during which three Marlboro regular filter cigarettes were smoked. See Figure 7 for a sketch of the room setup. The close agreement between measurements at all the three locations during the three experiments helps support the assumption of a spatially uniform concentration in the room, i.e., the room is “well-mixed”.

straight line yielded approximately the same ventilatory air exchange rate of  $\phi = 1.2$  air changes per hour (ach) at all locations for this experiment.

Table 1: Average CO Concentration (pptm) Measured in the Bedroom at Three Locations after Smoking of Three Successive Marlboro Regular Filter Cigarettes

Experiment No.	Corner Floor	Center of Room	Top of Ladder	Mean
1	5.62	6.81	5.90	6.11
2	5.18	6.30	5.61	5.70
3	4.19	5.16	3.88	4.41
Mean	5.00	6.09	5.13	5.41

The CO concentration time series, when averaged over each smoking episode, ranged from 3.88 pptm to 5.9 pptm, with an average for all episodes of 5.4 pptm (Table 1). The center of the room averaged about 1-1.2 pptm (21-23%) higher than the corner floor and about 0.7-1.3 pptm (19-33%) higher than the ceiling. One would expect a higher average concentration in the center, because the cigarette was smoked there within 12" of the CO monitor. It is unlikely that a person would spend several hours either at the two extreme locations – the corner floor or the ceiling – and the concentrations observed probably would differ by less than the 19-33% from the mean. The average exposure of a person inside the room probably would be closer to the overall mean of 5.4 pptm, because they would move around the room.

Baughman *et al.*<sup>15</sup> studied a chamber with 40 sampling points to determine how rapidly the concentrations at different points converge, and Mage and Ott<sup>16</sup>, in reviewing their research, suggest three different time phases for an indoor source: an “alpha-period” in which the source is emitting and the concentrations vary spatially, a “beta-period” in which the source is off but the room is not yet well-mixed, and a “gamma-period” in which the *coefficient of variation* (i.e., the ratio of the standard deviation to the mean) across all monitoring points in the room is less than 0.10, and the room is judged to be “well-mixed.” There were too few monitoring locations in our bedroom experiment to compute the coefficient of variation, but Table 1 shows that the concentration time series pattern after the cigarettes end is similar at the three locations. For a cigarette, the alpha-period is short relative to the other periods.

To estimate the cigarette mass emission rate, consider a previously published cigarette smoking time series model,<sup>9</sup> which expresses the *average concentration*  $\overline{x_A(T)}$  over time  $T$  as a function of the average source strength  $\overline{g_A(T)}$ , the instantaneous concentration  $x(T)$ , the volume  $v_A$ , and the air exchange rate  $\phi_A$ :

$$\frac{\overline{g_A(T)}}{\phi_A v_A} - \overline{x_A(T)} = \frac{x_A(T)}{T \phi_A} \quad (46)$$

At the end of the exponential decay period, we assume  $x_A(T) \cong 0$  so that

$$\frac{\overline{g_A(T)}}{\phi_A v_A} \cong \overline{x_A(T)} \quad (47)$$

The product of the average source emissions and the time  $T$  gives the total emissions  $m_{cig}$ , so multiplying both sides of Equation 47 by  $T\phi_A v_A$  gives:

$$m_{cig} = [\overline{g_A(T)}]T = [\overline{x(T)}]T\phi_A v_A \quad (48)$$

Substituting the values of 5.41 pptm,  $\phi_A = 1.2$  air changes per hour (ach),  $v_A = 25.7 \text{ m}^3$ , and the average experiment duration of 4.25 hours, we can compute the total source emissions for the cigarette experiment in the bedroom:

$$m_{cig} = (0.541 \text{ ppm}) \left( 1.145 \frac{\text{mg}}{\text{m}^3\text{-ppm}} \right) \left( 1.2 \frac{\text{air change}}{\text{hr}} \right) (4.25 \text{ hr}) \left( 25.7 \frac{\text{m}^3}{\text{air change}} \right) = 81.2 \text{ mg} \quad (49)$$

The resulting total CO emission of 81.2 mg is not very different from the total CO emission of 88 mg obtained by combining mainstream and sidestream smoke from Marlboro cigarettes from experiments in a chamber and an automobile and is similar to values reported in the literature.<sup>9</sup> Rosanno and Owens<sup>33</sup> report a CO source strength for the cigarette of 86 mg if mainstream and sidestream smoke are combined, which is close to our result. Notice that, at time  $t = 0$ , use of Equation 44 gives  $x(0) = (m_{cig})/v_b = 81.2 \text{ mg}/25.7 \text{ m}^3 = 3.16 \text{ mg}/\text{m}^3$  CO. This result converts to  $(3.16 \text{ mg}/\text{m}^3)(1 \text{ ppm}\cdot\text{m}^3/1.147 \text{ mg})(10 \text{ pptm}/\text{ppm}) = 27.6 \text{ pptm}$ , which is close to the peak concentrations observed for each cigarette in Figure 8.

### 3.2 Concentrations in Two Adjacent Rooms with Door Open

In another experiment, we closed the windows, left the door into the living room open, and smoked three Kentucky reference cigarettes (No. 2R1) one after another in the bedroom to provide a strong source. RSP concentrations were measured (2-min averages) in the living room and center of the bedroom using a Model 8510 piezobalance (TSI, Inc., St. Paul, MN). The operation and performance characteristics of this monitor, which measures mass concentrations of fine particles with a 3.5-micrometer cutpoint (PM<sub>3.5</sub>) at 2-minute averaging times, are described in greater detail in an earlier published paper on particle measurements in a tavern.<sup>11</sup> The CO sensor on the tall ladder (Location 3 in Figure 7) was relocated to the living room from the bedroom, but the other two bedroom sensor locations were unchanged and the door between the two rooms stayed open. Fine particle-bound polycyclic aromatic hydrocarbon (PPAH) concentrations were measured at the corner floor location of the bedroom using a real-time PAH monitor (EcoChem Technologies, Inc., West Hills, CA) that has been used in other ETS experiments.<sup>32</sup>

Although the RSP concentrations for the two adjacent rooms initially diverge, they rapidly come together after 45 minutes and remain very similar (Figure 9, top). Thus,

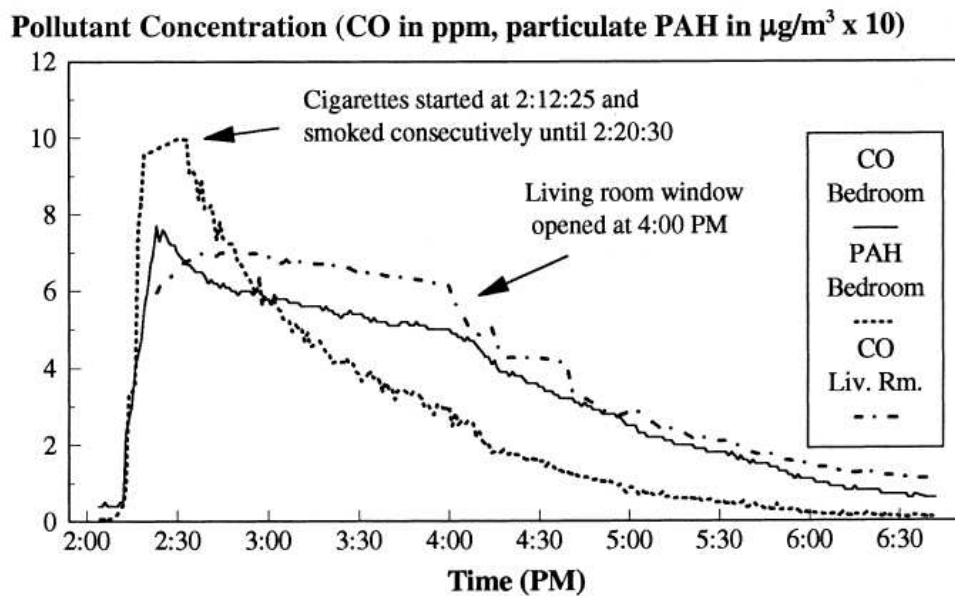
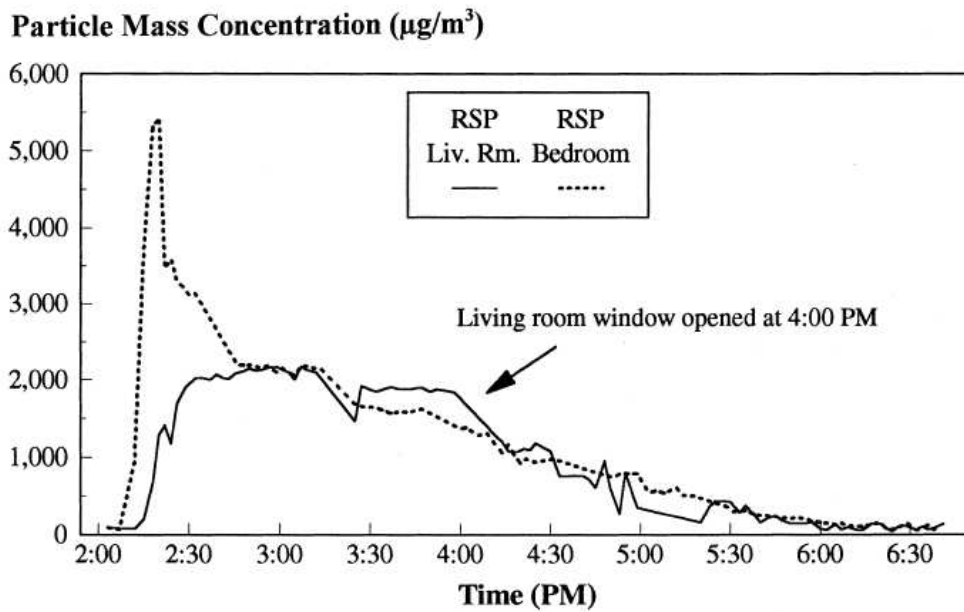


Figure 9: Respirable suspended particle (RSP) concentration (top) and carbon monoxide (CO) and particulate polycyclic aromatic hydrocarbon (PPAH) concentration (bottom) measured simultaneously in the bedroom and living room with the door open after three Kentucky No. 2R1 research cigarettes were smoked in the bedroom. A reading of "10" for PPAH should be divided by 10 to give  $1 \mu\text{g}/\text{m}^3 = 1,000 \text{ ng}/\text{m}^3$ .

with the door between the bedroom and living room wide open, the two adjacent rooms behave almost as a single compartment.

The RSP concentrations caused by the three Kentucky research cigarettes were extremely high, reaching a momentary peak concentration of  $5,500 \mu\text{g}/\text{m}^3$  in the bedroom. Indeed, the levels were so high that the three investigators found it necessary to open a living room window at 4:00 pm, and the effect of opening this window in changing the air exchange rate is evident (Figure 9, bottom). Unlike CO, both RSP and particulate PAH are deposited on surfaces, and PAH therefore shows a more rapid decay than CO in the bedroom. It should be noted that the Kentucky No. 2R1 research cigarettes have higher particulate emissions than ordinary retail cigarettes do.

### 3.3 Concentrations in Adjacent Rooms with Doors Almost Closed

To examine the relationships among the time series in several rooms, a cigar was smoked in the kitchen to provide a strong CO source, and the resulting CO concentrations were measured in the kitchen, living room, and bedroom. Long coaxial wire cables were extended into each room with Langan L15 CO sensors attached at the end, and CO concentrations on all three channels were logged using a DataBear<sup>TM</sup> data logger.<sup>29</sup> As before, precision operational amplifiers multiplied the voltages by 10 to increase the sensitivity.<sup>31</sup> The kitchen-to-living room door was open 3", and its position was locked in place by masking tape. The living room-to-bedroom door was closed, and all windows in the living room and bedroom were closed. The other doors to nearby rooms were closed with tape attached around all the doors, leaving only three rooms through which CO could readily move.

The concentrations observed in two of the three rooms after a cigar was smoked in the kitchen for 15 min (Figure 10) have the same general shapes as predicted by the two compartment model in Figure 5 with a source in Room A (kitchen) and the concentration observed in Room B (living room). More pollutant transfer occurs if the door is open wide (Figure 9) or open a crack (3" for the kitchen door in Figure 10) than if the door is closed entirely (bedroom concentration in Figure 10), because the closed door acts as a barrier to movement of air. Except for the closed bedroom door, the doors to all the other rooms of the house were sealed tightly, so most of the air and pollutant flow occurs in the two compartments represented by the kitchen and living room. Because of the importance of the door position and its effectiveness in shielding occupants of the home from ETS, it appears that additional research is needed to determine the effect of the door positions and window positions on the interzonal pollutant movement in real homes.

To apply the two compartment model's analytical solutions for rectangular source input, we must determine the values of all the parameters of the two compartment model. The volumes  $v_A$  and  $v_B$  are determined from physical measurement of the dimensions of the rooms, but we still require the interzonal flow rate parameters  $\alpha_{AB}$  and  $\alpha_{BA}$ , the air change rates  $\phi_A$  and  $\phi_B$ , and the source strength  $m_{source}$ . To find these values, we used a grid search method to find values of the 5 unknown parameters that yielded the minimum error. Values leading to negative flow rates were discarded. The error is de-

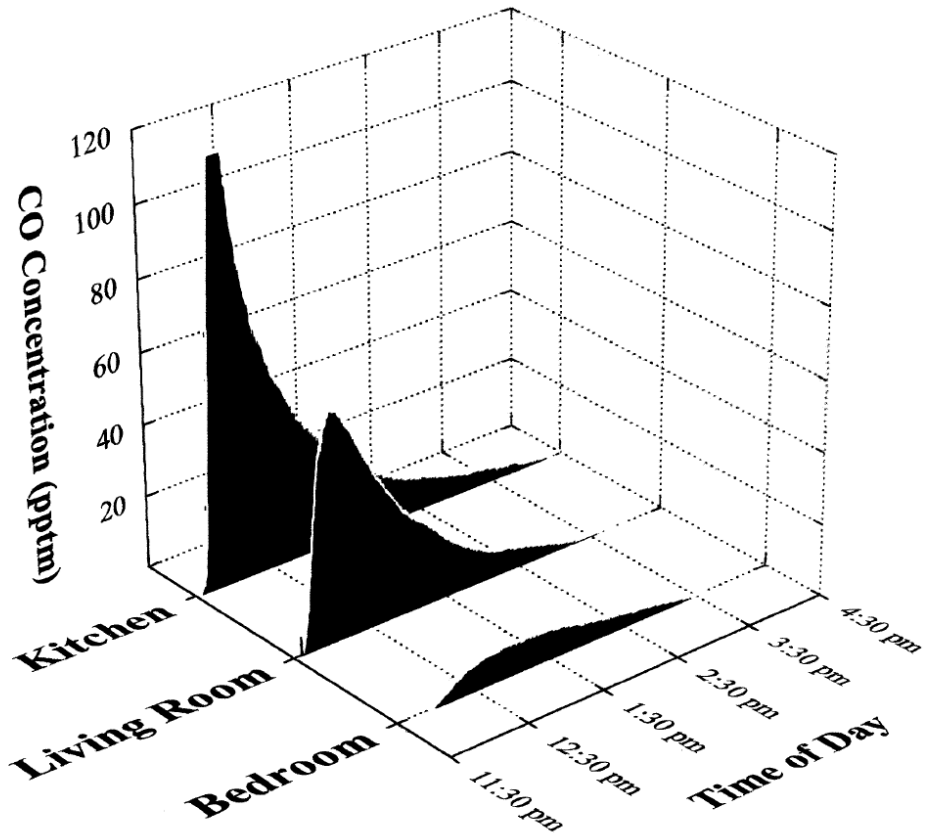


Figure 10: The carbon monoxide time series in three rooms of the house after a cigar was smoked in the kitchen. The kitchen door was open three inches and the bedroom window and door were closed.

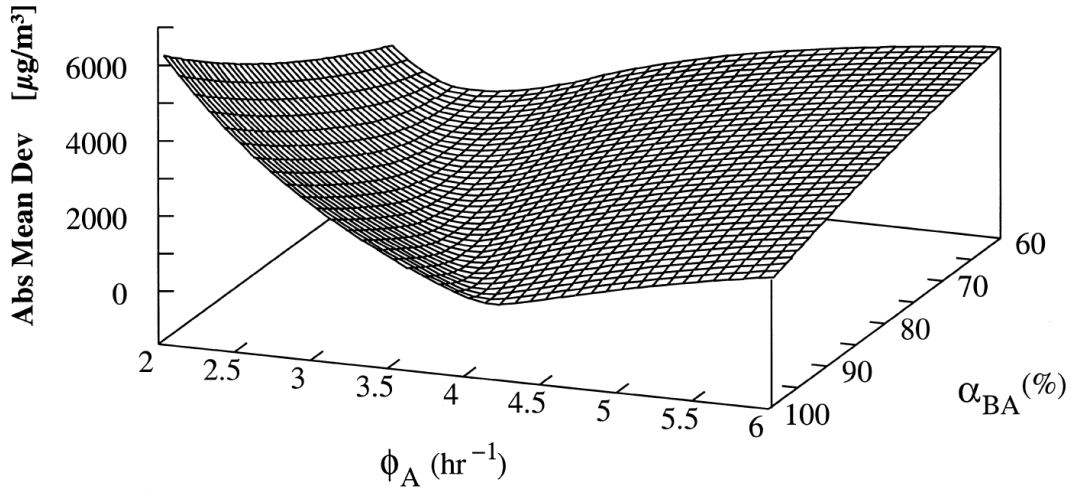


Figure 11: Example of a three-dimensional plot of the optimization error surface when two parameters, Room A's air exchange rate  $\phi_A$  and the interzonal flow factor  $\alpha_{BA}$  reflecting the proportion of air flow that Room A receives from Room B, are varied over a wide range. This error surface is the mean absolute deviation between the predicted and observed concentration time series, and a minimum occurs at  $\phi_A = 4 \text{ h}^{-1}$  and  $\alpha_{BA} = 0.95$ , the lowest point of a shallow channel.

defined as the mean absolute deviation between the model-predicted concentration curve and the measured concentration curve. In the grid search method, the parameter values begin with an initial starting point and then small increments are subtracted or added iteratively to each parameter to reduce the error. At the end of a number of computer iterations, the final values of the parameters are those giving the smallest error. Although it is not possible to plot the error surface in 5 dimensions, we can give an example of the error surface plotted in 3 dimensions as a function of the air exchange rate in the kitchen  $\phi_A$  and the proportion of the air flow that Room A receives from Room B,  $\alpha_{BA}$  (Figure 11). This graph shows a minimum pathway (or channel) in the error surface as well as flat areas with high uncertainty in the estimated parameter values (i.e., the values corresponding to the minimum error point). In the flat regions, there is uncertainty about the values of the parameters. For this particular surface, a fairly narrow channel exists from moderate values of  $\phi_A$  and  $\alpha_{BA}$  to their optimum values of  $4 \text{ hr}^{-1}$  and  $0.95$ , respectively.

Figure 12 shows the two compartment model fit to the complete CO time series in the kitchen and the living room of the small residence (Figure 6), with a cigar smoked for 15 min in the kitchen. This fit represents a minimum value in the error surface. The grid search minimization approach gave the following values of the parameters: air change rates of  $\phi_A = 4 \text{ hr}^{-1}$  in the kitchen and  $\phi_B = 4.6 \text{ hr}^{-1}$  in the living room; interzonal flow ratios of  $\alpha_{BA} = 0.95$  for the kitchen and  $\alpha_{AB} = 0.62$  for the living room, and  $g_{source} = 60 \text{ mg/min}$  for 15 min, giving a source strength of  $m_{source} = (60 \text{ mg/min})(15 \text{ min}) = 900 \text{ mg}$ , which is comparable to the CO source strengths observed in other cigar experiments.<sup>29</sup>

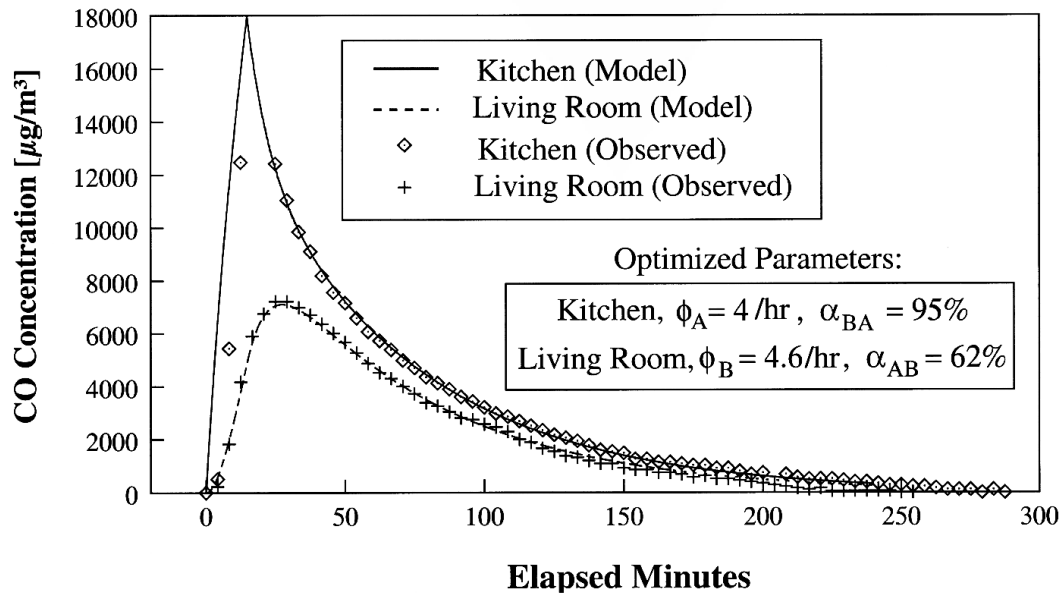


Figure 12: Comparison of carbon monoxide (CO) concentration predicted by the two-compartment model with CO concentration measured in the kitchen and living room of the house in Menlo Park, CA after a cigar was smoked for 15 min in the kitchen. The values of the five parameters were obtained by a grid search optimization method. The resulting air exchange rates for the kitchen and living room were  $\phi_A = 4 \text{ h}^{-1}$  and  $\phi_B = 4.6 \text{ h}^{-1}$ , respectively. The interzonal flow percentages were 95% for the kitchen, i.e., the proportion of air that the kitchen receives from the living room is 0.95, and 62% for the living room, i.e., the proportion of air that the living room receives from the kitchen is 0.62. The cigar's source emission rate was found to be  $\text{g}_{\text{source}} = 60 \text{ mg}/\text{min}$ , which is similar to the CO emission rates for cigars reported elsewhere.<sup>29</sup>

The two compartment model fits the experimental data reasonably well throughout the duration of the experiment, except for the beginning of the source room time series where it appears that nonuniform mixing in the kitchen (Room A) during the alpha-period caused a decreased concentration. The living room concentration time series (Room B) fits very well, even at the very beginning. The two rooms obviously behave as two compartments despite relatively high air change rates (4-6 hr<sup>-1</sup>) and fairly high interzonal flow rate (95% of the air entering the kitchen is from the living room and 62% of the air entering the living room is from the kitchen).

Calculating the overall air change rate with the outdoor air for the two rooms combined shows that it is much lower than the individual room air change rates of  $\phi_A = 4 \text{ hr}^{-1}$  and  $\phi_B = 4.6 \text{ hr}^{-1}$ . For example, the total volumetric air flow in Room A is  $w_A = v_A \phi_A = (34 \text{ m}^3)(4 \text{ hr}^{-1}) = 136 \text{ m}^3/\text{hr}$ , and the total volumetric air flow in Room B is  $w_B = v_B \phi_B = (36 \text{ m}^3)(4.6 \text{ hr}^{-1}) = 165.6 \text{ m}^3/\text{hr}$ . Using the formulas for  $\alpha_{AB}$  and  $\alpha_{BA}$  in Equations 9 and 11, we calculate the interzonal flow rates as  $w_{AB} = (w_{AB} + w_{OB})\alpha_{AB} = w_B \alpha_{AB} = (165.6 \text{ m}^3)(0.62) = 102.7 \text{ m}^3/\text{hr}$  and  $w_{BA} = (w_{BA} + w_{OA})\alpha_{BA} = w_A \alpha_{BA} = (136 \text{ m}^3)(0.95) = 129.2 \text{ m}^3/\text{hr}$ . As discussed in the text after Equations 7–12, the total air flow for rooms A and B with the outdoors and other rooms, minus internal flows between them is:  $w = w_A + w_B - (w_{BA} + w_{AB}) = 136 + 165.6 - (102.7 + 129.2) = 301.6 - 221.9 = 69.7 \text{ m}^3/\text{hr}$ . Therefore, the overall air change rate for the two rooms is  $\phi = w/(v_A + v_B) = 69.7/(34 + 36) = 0.995 \text{ hr}^{-1}$ . This result is close to 1 air change per hour, typical of the air change rates for a small California residence with the external doors and windows closed. Thus, the higher air change rates for the individual rooms reflect the more rapid air flow occurring between the kitchen and the living room when the door between these two adjacent rooms is open 3" (7.6 cm).

These results illustrate that one can determine all the parameters for the two compartment model in a single experiment, although the relatively flat error surface in Figure 11 suggests that a range of parameter values around the optimal values would cause almost as good a fit to the data as the optimal values. One reason that compartmental indoor air quality experiments often use two or more tracer gases instead of the single gas used here is an attempt to reduce uncertainty in the parameter values. However, the flat error surface has a practical advantage: slight errors in the parameter values do not impair the excellent fit of the predicted time series to the measured concentration time series in both rooms.

## 4 Summary and Conclusions

In this paper, we use Laplace transforms to represent indoor sources of air pollution with emission rates that begin and end at specific times, and solve the basic indoor differential equations algebraically for one and two compartments for impulse, step, and rectangular source time functions. We apply the solutions to a real house where the predicted and continuously measured concentrations are compared in several rooms. The predicted time series showed good agreement with the continuous measurements measured in this

home. Our approach yielded analytical expressions for the slopes, maxima, and points of inflection of the predicted curves that may be of practical use in other indoor air quality studies. These analytical expressions are an alternative to Runge-Kutta methods that take tiny iterative steps on a computer using discrete versions of the same differential equations.

Although this paper presents analytical solutions for the impulse, step, and rectangular source functions, there are other common indoor source functions for which these general methods are suitable. These methods, illustrated here for ETS sources, can be applied to any indoor source whose Laplace transform can be found.

Because the duration of a cigarette often is brief relative a house's residence time  $\tau$  (i.e., the reciprocal of the air change rate) the cigarette source sometimes can be represented by an impulse function instead of a rectangular source function. With this approximation, the total amount of pollutant emitted by the cigarette, or its total mass source strength  $m_{cig}$ , is the product of the volume of the compartment  $v$  and the estimated maximum concentration. This result agrees with common sense: if a pollutant  $m_{cig}$  suddenly dispersed uniformly over a single compartment's mixing volume  $v$ , then the resulting initial maximum concentration will be approximately equal to the mass released divided by the volume, or  $(m_{cig})/v$ .

For the single-compartment case with an impulse, step, or rectangular source time function, the analytical solution is a single exponential function of time. For the two compartment case, the analytical solution is the difference between two exponential functions of time. Analytical solutions have been derived for the maxima and can be applied using a hand calculator. The two eigenvalues for the two compartment solutions, which depend on the physical volume, air change rates, and interzonal flow factors of the rooms, determine the times of occurrence of the maximum concentrations and points of inflection for the predicted concentration time series.

In our experiments using continuous measurements in three rooms of a small, detached home, we found that two rooms with an open door between them behaved as a single compartment. In contrast, two adjacent rooms with the door tightly closed or opened slightly (for example, 3" or less) behaved as two separate compartments. Our experiments also showed that the position of the doors and windows had a large effect on the indoor concentrations in different rooms. Our results suggest that a smoker indoors may be able to confine the ETS generated in a particular part of the home by closing the doors and opening windows in the room in which the smoking takes place, thereby reducing the ETS exposure of other residents. More research is needed on the effectiveness of this indoor "isolation" effect.

Howard-Reed *et al.*<sup>18</sup> studied the effect of window positions on the air change rates of two homes, and it appears that future research should focus systematically on the effect of other similar factors in the home. These factors include opening and closing internal doors, the compartmental effect of hallways, the effect of fans and ventilation systems, and other physical and human activities that may influence indoor pollutant concentrations. The increasing use of real-time measurement methods in indoor residential settings<sup>36</sup> promises to provide important new insights into the factors affecting indoor air

and human exposure to environmental pollutants in the home. Indoor predictions based on validated models and indoor source strengths allow the findings from one home to be extended and generalized to other homes.

## Acknowledgments

This research was supported in part by the Cigarette and Tobacco Surtax Fund of the State of California through the Tobacco-Related Disease Research Program of the University of California (Grant No. 6RT-0118). This work was also supported by the U.S. Environmental Protection Agency (EPA) National Exposure Research Laboratory through Interagency Agreement DW-988-38190-01-0 with the U.S. Department of Energy (DOE) under Contract Grant No. DE-AC03-76SF00098 at Lawrence Berkeley National Laboratory (LBNL) and through an LBNL subcontract to Stanford University.

## References

1. Klepeis, N.E., Nelson, W.C., Ott, W.R., Robinson, J.P., Tsang, A.M., Switzer, P., Behar, J.V., Hern, S.C., Engelmann, W.H. (2001) "The National Human Activity Pattern Survey (NHAPS): A Resource for Assessing Exposure to Environmental Pollutants," *Journal of Exposure Analysis and Environmental Epidemiology*, Vol 11(3), pp. 231-252.
2. Wadden, R.A. and Scheff, P.A. *Indoor Air Pollution: Characterization, Prediction, and Control*, John Wiley & Sons (1983).
3. Ott, W.R. (1999) "Mathematical Models for Predicting Indoor Air Quality from Smoking Activity," *Environmental Health Perspectives*, Vol. 107, Supplement 2, May 1999, pp. 375-381.
4. McKone, T.E. "Household Exposure Models," *Toxicology Letters*, Vol. 49. pp. 321-339 (1989).
5. Wilkes, C.R., Small, M.J., Andelman, J.B., Giardino, N.J., and Marshall, J. "Inhalation Exposure Model for Volatile Chemicals from Indoor Uses of Water," *Atmos. Environ.*, Vol. 26A, No. 12, pp. 2227-2236 (1992).
6. Axley, J.W., and Lorenzetti, D. "IAQ Modeling Using STELLA<sup>TM</sup>: A Tutorial Introduction," Building Technology Program, Massachusetts Institute of Technology, (Fall 1991).
7. Sparks, L.E., Tichenor, B.A., White, J. B., Chang, J. and Jackson, M.D. "Verification and Uses of the Environmental Protection Agency (EPA) Indoor Air Quality Model," Paper No. 91-62.12 presented at the 84<sup>th</sup> Annual Meeting of the Air and Waste Management Association, British Columbia, June 16-21 (1991).

8. Nagda, N., ed., *Modeling of Indoor Air Quality and Exposure*, ASTM STP 1205, American Society for Testing and Materials, West Conshohocken, PA (1993).
9. Ott, W., Langan, L., and Switzer, P. "A Time Series Model for Cigarette Smoking Activity Patterns: Model Validation for Carbon Monoxide and Respirable Particles in a Chamber and an Automobile," *J. Expos. Anal. & Environ. Epidemiology*, Vol. 2, Suppl. 2, pp. 175- 200 (1992).
10. Klepeis, N.E., Ott, W.R. and Switzer, P. "A Multiple-Smoker Model for Predicting Indoor Air Quality in Public Lounges," *Environ. Sci. & Technol.*, Vol 30, No. 9, pp. 2813-2820 (1996).
11. Ott, W., Switzer, P. and Robinson, J. "Particle Concentrations Inside a Tavern Before and After Prohibition of Smoking: Evaluating the Performance of an Indoor Air Quality Model," *J. Air & Waste Manag. Assoc.*, Vol. 45, No. 12, pp. 2-16 (1996).
12. Miller, S.L., Leiserson, K., and Nazaroff, W.W., "Nonlinear Least-Squares Minimization Applied to Tracer Gas Decay for Determining Airflow Rates in a Two-Zone Building," *Indoor Air*, Vol. 7, pp. 64-75 (1997).
13. Miller, S.L. and Nazaroff, W.W., "Environmental Tobacco Smoke Particles in Multi-zone Indoor Environments," *Atmospheric Environment*, Vol. 35, pp. 2053-2067 (2001).
14. Rogers, L.C. (1980) "Air Quality Levels in a Two-Zone Space," *ASHRAE Transactions*, vol. 86, Part 2, pp. 92-98.
15. Baughman, A.V., Gadgil, A.J., and Nazaroff, W.W. "Mixing of a Point Source Pollutant by Natural Convection Flow Within a Room," *Indoor Air*, Vol. 4, pp. 114-122 (1994).
16. Mage, D.T., and Ott, W.R. "The Correction for Nonuniform Mixing in Indoor Microenvironments," in Tichenor, B.A., *Characterizing Indoor Air Pollution and Related Sink Effects*, STP-1287, pp. 263-278, ASTM, West Conshohocken, PA (1996).
17. Klepeis, N.E., "Validity of the Uniform Mixing Assumption: Determining Human Exposure to Environmental Tobacco Smoke," *Environmental Health Perspectives*, 1999. Vol. 107, pp. 357-363.
18. Howard-Reed, C., Wallace, L.A., and Ott, W.R., "The Effect of Opening Windows on Air Change Rates in Two Homes," accepted for publication in the *Journal of the Air and Waste Management Association* 82:147-159 (2002).
19. Pandian, M., Behar, J., Ott, W., Wallace, L., Wilson, A.L., Colome, S. and Koontz, M. "Correcting Errors in the Nationwide Data Base of Residential Air Exchange Rates," *J. Expos. Anal. & Environ. Epidem.* 8(4):577-586 (1998).

20. Dorf, R.C., and Bishop, R.H. "Introduction to Control Systems," Addison-Wesley, Reading, MA (1996).
21. D'Azzo, J.J., *Linear Control System Analysis and Design: Conventional and Modern*, Fourth Edition, McGraw Hill (New York 1995).
22. D'Azzo, J. and Houpis, C.J. *Feedback Control System Analysis and Synthesis*, McGraw-Hill (New York 1966).
23. Franklin, G.F., Powell, J.D., and Emani-Naeini, A., *Feedback Control of Dynamic Systems*, Third Edition, Addison-Wesley Publishing Co. (Reading, MA 1994).
24. Gujic', Z., and M. Lelic', *Modern Control Systems Engineering*, Prentice-Hall, London, (1996).
25. Nise, N.S., *Control Systems Engineering*, Second Edition, The Benjamin/Cummings Publishing Co. (Redwood City, CA 1995).
26. Blanchard, P., Devaney, R.L., and Hall, G.R. (1997) *Differential Equations*, Brooks/Cole Publishing Co., Pacific Grove, CA.
27. Bugl, P. (1995) *Differential Equations: Matrices and Models*, Prentice Hall, Englewood Cliffs, NJ.
28. Edwards, C.H., and Penney, D.E. (1996) *Differential Equations and Boundary Value Problems*, Prentice Hall, Upper Saddle River, NJ.
29. Klepeis, N.E., Ott, W.R., and Repace, J.L., "The Effect of Cigar Smoking on Indoor Levels of Carbon Monoxide and Particles," *Journal of Exposure Analysis and Environmental Epidemiology*, Vol. 9, pp. 622-635 (1999).
30. Ott, W., and Switzer P. "Analytical Solutions to the two compartment Indoor Model by Laplace Transforms," Research Report, Department of Statistics, Sequoia Hall, Stanford, CA 94305 (2002).
31. Langan, L. "Portability in Measuring Exposure to Carbon Monoxide," *J Expos. Anal. and Environ. Epidemiology*, Supplement 1, pp. 223-239 (1992).
32. Ott, W.R., Vreman, H.J., Switzer, P., and Stevenson, D.K. "Evaluation of Electrochemical Monitors for Measuring Carbon Monoxide Concentrations in Indoor, In-Transit, and Outdoor Microenvironments," in "Measurement of Toxic and Related Air Pollutants," Proceedings of the U.S.EPA/A&WM International Symposium, Research Triangle Park, NC, Air and Waste Management Association, Pittsburgh, PA, VIP-50, pp. 172-177 (1995).
33. Rosanno, A.J. and Owens, D.F. "Design Procedures to Control Cigarette Smoke and Other Air Pollutants," *ASHRAE Transactions*, Vol. 75, pp. 93-102 (1969).

34. Ott, W.R., Wilson, N.K., Klepeis, N.E., and Switzer, P. "Real-time Monitoring of Polycyclic Aromatic Hydrocarbons and Respirable Suspended Particles from Environmental Tobacco Smoke in a Home," in "Measurement of Toxic and Related Air Pollutants," Proceedings of the U.S.EPA/A&WM International Symposium, Durham, NC, EPA/600/R-94/136, Air and Waste Management Association, Pittsburgh, PA, VIP-39, pp. 887-892 (1994).
35. Wilson, N.K., Barbour, R.K., Chuang, J.C., and Mukund, R. "Evaluation of a Real-Time Monitor for Fine Particle-Bound PAH in Air," *Polycyclic Aromatic Compounds*, Vol. 5, pp. 167-174 (1994).
36. Long, C.M., Suh, H.H., and Koutrakis, P. "Characterization of Indoor Particle Sources Using Continuous Mass and Size Monitors," *J. Air and Waste Management Association*, Vol. 50, pp. 1236-1250 (July 2000).

## A Laplace Transforms of the Source Time Functions in this Paper

The general Laplace transform function  $X(s)$  of the function  $x(t)$  is defined by:

$$L\{x(t)\} = X(s) = \int_0^{\infty} x(t)e^{-st} dt \quad (50)$$

For the Heaviside function  $x(t) = u_a(t)$ , Laplace transform is derived as

$$\begin{aligned} L\{u_a(t)\} &= \int_a^{\infty} u_a(t)e^{-st} dt = \lim_{b \rightarrow \infty} \int_a^b u_a(t)e^{-st} dt \\ &= \lim_{b \rightarrow \infty} \frac{b}{a} \left[ \frac{1}{-s} e^{-st} \right] = 0 - \frac{1}{-s} e^{-at} = \frac{e^{-at}}{s} \quad (51) \end{aligned}$$

If the Heaviside function is shifted to the origin, substituting  $t = 0$  into Equation 51 gives  $e^0 = 1$  for a Heaviside function that begins at  $t = 0$ :

$$L\{u_0(t)\} = \frac{1}{s} \quad (52)$$

For the exponential function  $x(t) = e^{-\alpha t}$  for  $t \geq 0$ , where  $\alpha$  is the decay parameter, the Laplace transform of a decaying exponential function is derived as

$$\begin{aligned}
L\{e^{-\alpha t}\} &= \int_0^{\infty} e^{-\alpha t} e^{-st} dt = \lim_{b \rightarrow \infty} \int_0^b e^{-(\alpha+s)t} dt \\
&= \lim_{b \rightarrow \infty} \left[ -\frac{1}{\alpha+s} e^{-(\alpha+s)t} \right]_0^b = 0 + \frac{1}{\alpha+s} e^0 = \frac{1}{\alpha+s} \quad (53)
\end{aligned}$$

## B Laplace Approaches for Solving Differential Equations

Given a function  $x(t)$  with Laplace transform  $L\{x\}$ , the Laplace transform of  $dx/dt$  is

$$L\left\{\frac{dx}{dt}\right\} = sL\{x\} - x(0) \quad (54)$$

$$\begin{aligned}
L\left\{\frac{d^2x(t)}{dt^2}\right\} &= sL\left\{\frac{dx(t)}{dt}\right\} - x'(0) = s[sL\{x(t)\} - x(0)] - x'(0) \\
&= s^2L\{x(t)\} - sx(0) - x'(0) \quad (55)
\end{aligned}$$